ARMY RESEARCH LABORATORY

Failure Engineered Heavy Metal Penetrators, Phase I, SBIR

R. Cavalleri, W. Tiarn, and
D. Nicholson

ARL-CR-5 December 1992

prepared by

Applied Technology Associates, Inc.
Orlando, FL

and

University of Central Florida
Orlando, FL

under contract

DAAL04-92-C-0007

REPORT DOCUMENTATION PAGE

Form Approved
OMB No. 0704-0188

1. AGENCY USE ONLY *(Leave blank)*

2. REPORT DATE
December 1992

3. REPORT TYPE AND DATES COVERED
Final Report-1/1/92 - 7/31/92

4. TITLE AND SUBTITLE
FAILURE ENGINEERED HEAVY METAL PENETRATORS, PHASE I, SBIR

5. FUNDING NUMBERS
Contract No. DAAL04-92-C-0007

6. AUTHOR(S)
R. Cavalleri* and W. Tiarn,* and D. Nicholson†

7. PERFORMING ORGANIZATION NAME(S) AND ADDRESS(ES)
*Applied Technology Associates Inc., Orlando, FL
†Univ. of Central Florida, Orlando, FL

8. PERFORMING ORGANIZATION REPORT NUMBER

9. SPONSORING/MONITORING AGENCY NAME(S) AND ADDRESS(ES)
U.S. Army Research Laboratory
Watertown, MA 02172-0001
ATTN: AMSRL-OP-PR-WT

10. SPONSORING/MONITORING AGENCY REPORT NUMBER
ARL-CR-5

11. SUPPLEMENTARY NOTES
Robert J. Dowding, COR

12a. DISTRIBUTION/AVAILABILITY STATEMENT
Approved for public release; distribution unlimited.

12b. DISTRIBUTION CODE
A

13. ABSTRACT *(Maximum 200 words)*
The use of a layered tungsten penetrator as a replacement for depleted uranium in kinetic energy penetrators was investigated. The penetrator was fabricated using strips of tungsten which were vacuum brazed to form a single part. Two filler metals were investigated, copper and nickel along with built in mechanical shear lines. The objective of the shear line was to act as a fault line along which the penetrator would fracture. A limited parametric study of layered penetrator configuration was conducted with the EPIC-2 computer code. The code was used to obtain estimates of the effect of tungsten layer thickness on penetration ability. Tests were conducted at the U.S. Army Materials Technology Laboratory, presently U.S. Army Research Laboratory, Materials Directorate, on twelve .30 inch diameter penetrators. The test results indicated that the thin layer penetrator performed better than the thick layer. Also the nickel braze material appeared to perform better than the copper. Combination of the thin layer with a nickel filler metal may potentially result in a penetrator with better performance than that of existing tungsten alloy penetrators.

14. SUBJECT TERMS
Penetrators, Kinetic energy penetrators, Tungsten alloy penetrators, Vacuum brazing, and Laminates

15. NUMBER OF PAGES
43

16. PRICE CODE

17. SECURITY CLASSIFICATION OF REPORT	18. SECURITY CLASSIFICATION OF THIS PAGE	19. SECURITY CLASSIFICATION OF ABSTRACT	20. LIMITATION OF ABSTRACT
Unclassified	Unclassified	Unclassified	UL

NSN 7540-01-280-5500

Standard Form 298 (Rev. 2-89)
Prescribed by ANSI Std. Z39-18
298-102

TABLE OF CONTENTS

LIST OF FIGURES

LIST OF TABLES

ABSTRACT

The use of a layered tungsten penetrator as a replacement for depleted uranium in kinetic energy penetrators was investigated. The penetrator was fabricated using strips of tungsten which were vacuum brazed to form a single part. Two filler metals were investigated, copper and nickel along with built in mechanical shear lines. The objective of the shear line was to act a fault line along which the penetrator would fracture. A limited parametric study of layered penetrator configuration was conducted with the EPIC-2 computer code. The code was used to obtain estimates of the effect of tungsten layer thickness on penetration ability. Tests were conducted at the Army Materials Technology Laboratory on twelve .30-inch diameter penetrators. The test results indicated that the thin layer penetrator performed better than the thick layer. Also the nickel braze material appeared to perform better than the copper. Combination of the thin layer with a nickel filler metal may potentially result in a penetrator with better performance than that of existing tungsten alloy penetrators.

RESULTS OF PHASE I WORK

SUMMARY

It is desirable to use a tungsten alloy to replace depleted uranium as the penetrator in kinetic energy weapons. A problem with the use of tungsten is its deformation as it penetrates the target. The tungsten forms a mushroom shaped cap as shown in Figure 1 which increases its drag and decreases its penetration capability. Used by itself tungsten is a brittle metal and fractures unless it is alloyed with other metals. Typical metals used in tungsten alloys are copper, iron, nickel and silver. They permit the resulting alloy to be machined. When used as a kinetic energy penetrator the tungsten has a tendency to deform giving a blunt nose as it progresses through the target. This results in a reduction of the armor penetration capability for the tungsten penetrator. This does not happen with depleted uranium. The uranium has the ability to self sharpen as its penetrates the target.

The use of a layered tungsten penetrator as shown in Figure 2 was investigated. The penetrator was fabricated using strips of tungsten which were vacuum brazed to form a single part. Depending on the filler metal used as the braze material, the strength of the shear line can be varied. Included in some of the penetrators fabricated were the use of built in mechanical shear lines to cause the penetrator to self sharpen as it progresses through the target.

The objective of the work was to develop a failure engineered tungsten alloy penetrator. In the selection of the penetrator configuration use was made of the EPIC-2 computer code. This code has in its data base copper and nickel, which were considered as the filler metal brazing material. It was attempted to use the code to obtain estimates of the effect of filler metal thickness and tungsten thickness on penetration ability. Due to limitations of the data in the materials data base of the code, the results of the code predictions were limited. The effect of tungsten thickness was obvious, but the effect of which filler material was better was inconclusive.

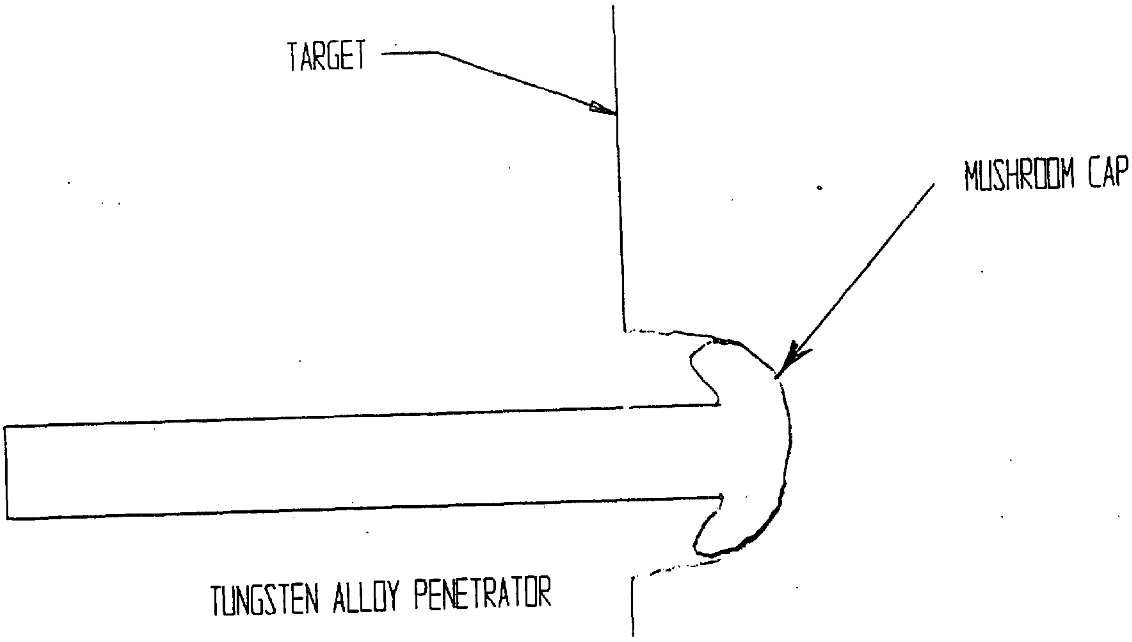

TYPICAL TUNGSTEN PENETRATOR DEFORMATION
FIGURE 1

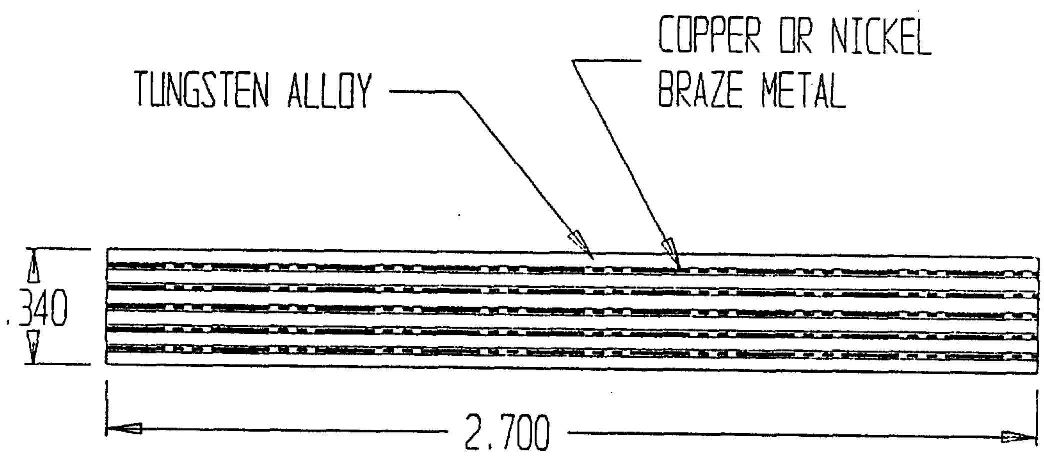

TYPICAL LAYERED TUNGSTEN PENETRATOR CONFIGURATION
FIGURE 2

PENETRATOR IMPACT ANALYSIS

The EPIC-2 computer code has the ability to evaluate kinetic energy penetrator performance. This computer code was used in an attempt to determine the effect of braze metal selection and tungsten thickness. The configuration for a six layer penetrator is shown in Figure 3a. The tungsten thickness is .050 inches and the braze metal thickness is .0025 inches. The nine layer configuration is shown in Figure 3b. The tungsten thickness is .030 and the braze metal thickness is .0025. The code can not analyze a two dimensional layered projectile. Thus the configurations analyzed are axisymmetric. The code results should still be indicative of the effects of tungsten thickness and braze metal selection.

To obtain a comparison of the effect of penetrator material, a pure copper and a pure tungsten case were first analyzed. The results for these cases are shown in Figure 4. At the time 10.0 $\times 10^{-6}$ seconds there is not much difference between the two results. At a later time of 20.0 $\times 10^{-6}$ seconds, the tungsten has spread to a larger diameter than the copper. The time step is not constant for each cycle and as a result the number of cycles does not have a one to one correlation with the elapsed time.

The initial penetrator was symmetrical about a tungsten layer. These results, shown in Figure 5 indicated that the braze metal junction in the center of the penetrator causes a failure at this location before the edge fails. This is contrary to the objective being sought. This case was modified so that the projectile was symmetrical about a tungsten layer.

Several configurations were analyzed using the EPIC-2 code. Nickel alloy and pure OFHC copper braze metal were employed. The physical and mechanical properties used were correct for each braze metal but the lower and upper failure limits were the same for both metals, as a result there is no difference between the copper and nickel penetrator deformation results. The results are shown in Figures 6a, 6b, 6c and 6d. The tungsten thickness is .030 and the braze metal thickness is .0025. The table below lists the cases that were analyzed using the EPIC-2 computer code.

TABLE 1 EPIC-2 COMPUTER RUNS

RUN NUMBER	TUNGSTEN THICKNESS (INCHES)	DESCRIPTION
1	.050	6 LAYER CU BRAZE
2	.030	9 LAYER CU BRAZE
3	.050	6 LAYER NI BRAZE
4	.030	9 LAYER NI BRAZE

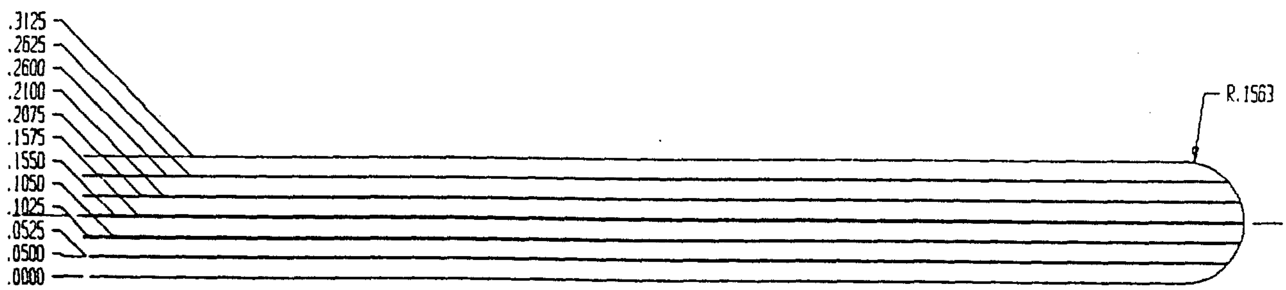

SIX LAYER PENETRATOR CONFIGURATION
FIGURE 3A

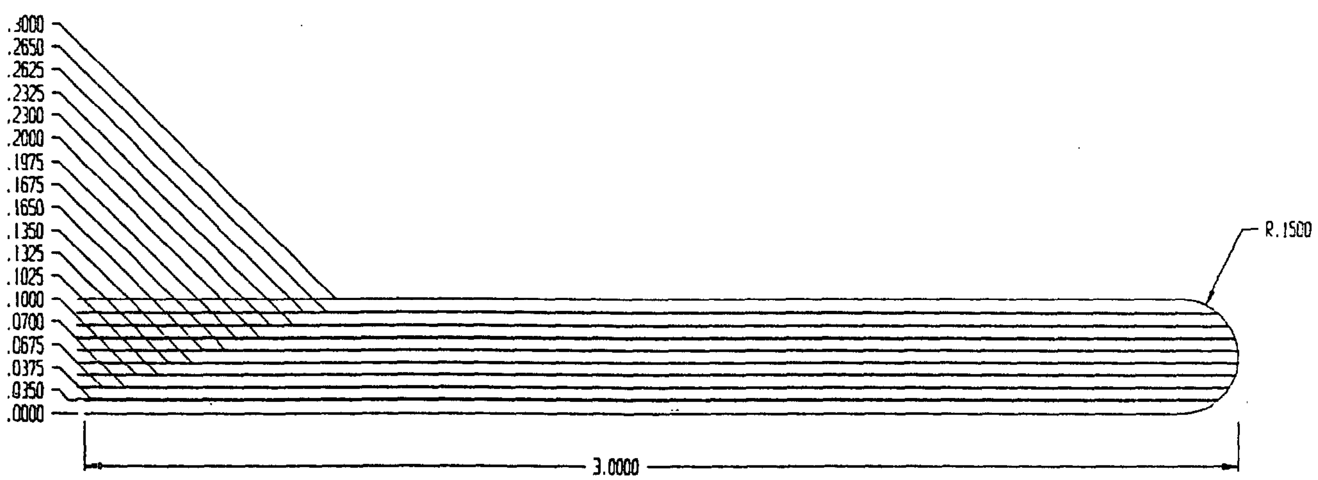

NINE LAYER PENETRATOR CONFIGURATION
FIGURE 3B

LAYERED PENETRATOR CONFIGURATIONS
FIGURE 3

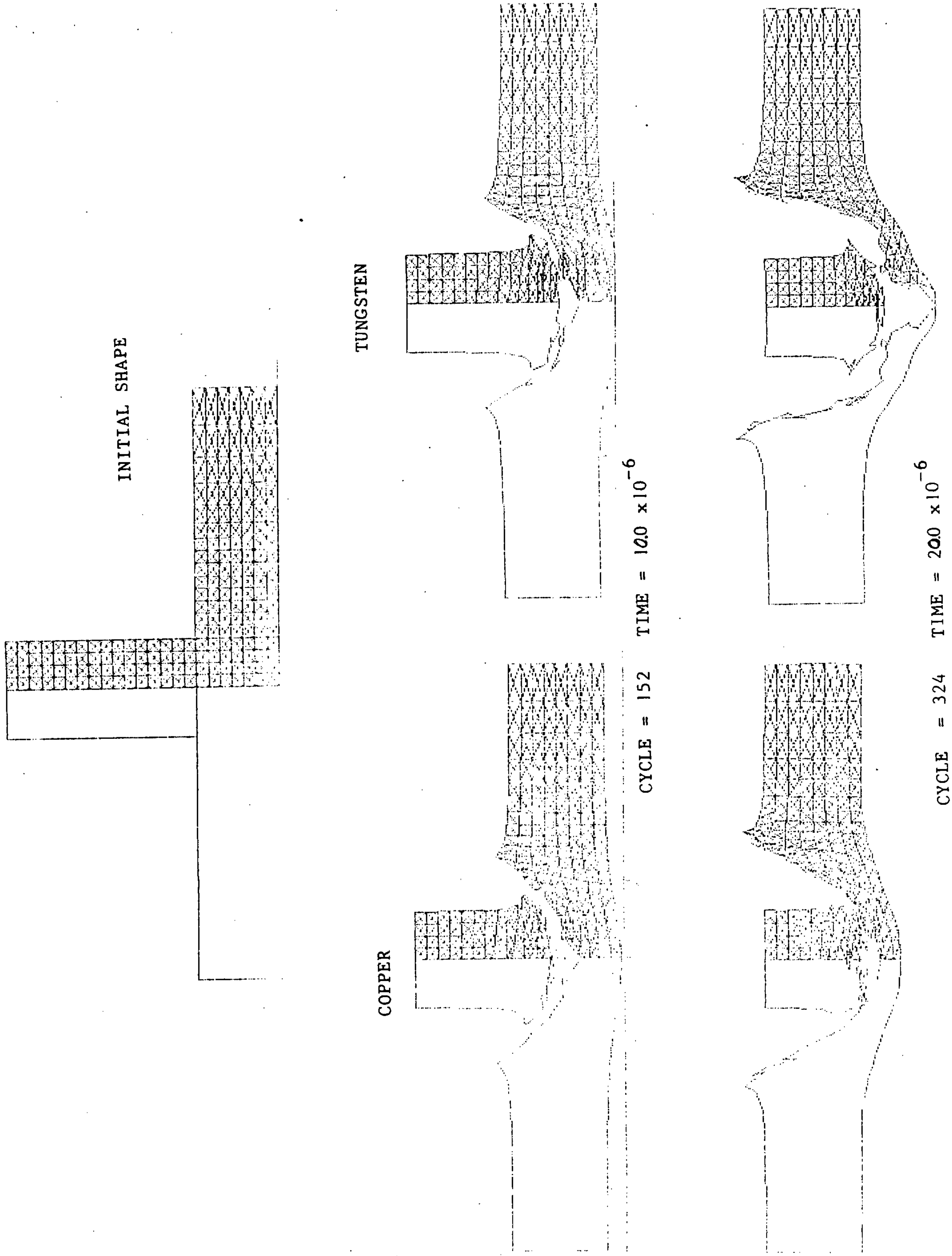

COMPARISON OF EPIC RESULTS FOR COPPER AND TUNGSTEN PENETRATORS
FIGURE 4

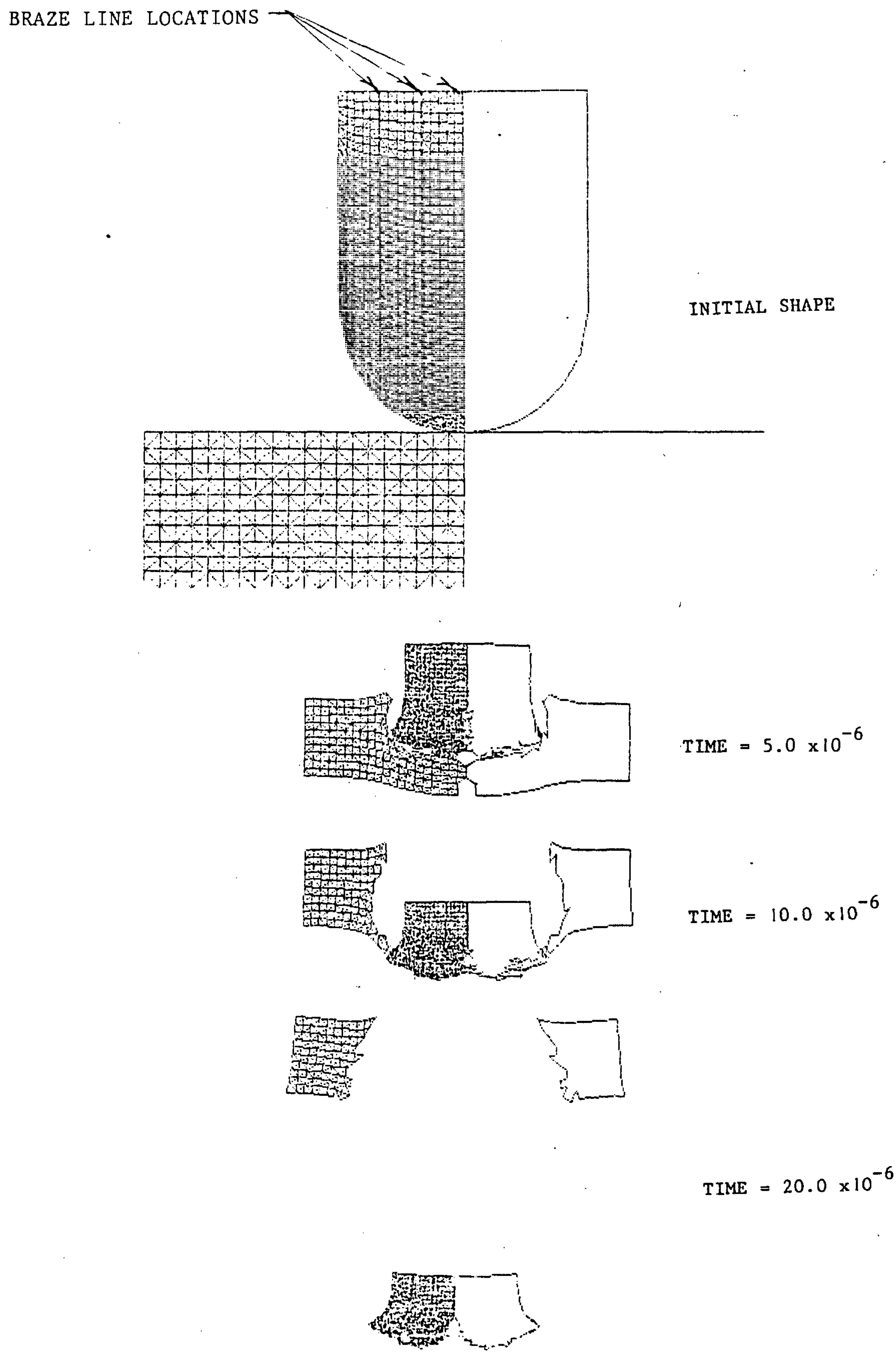

SIX LAYER BRAZE LINE SYMMETRY PENETRATOR EPIC RESULTS
FIGURE 5

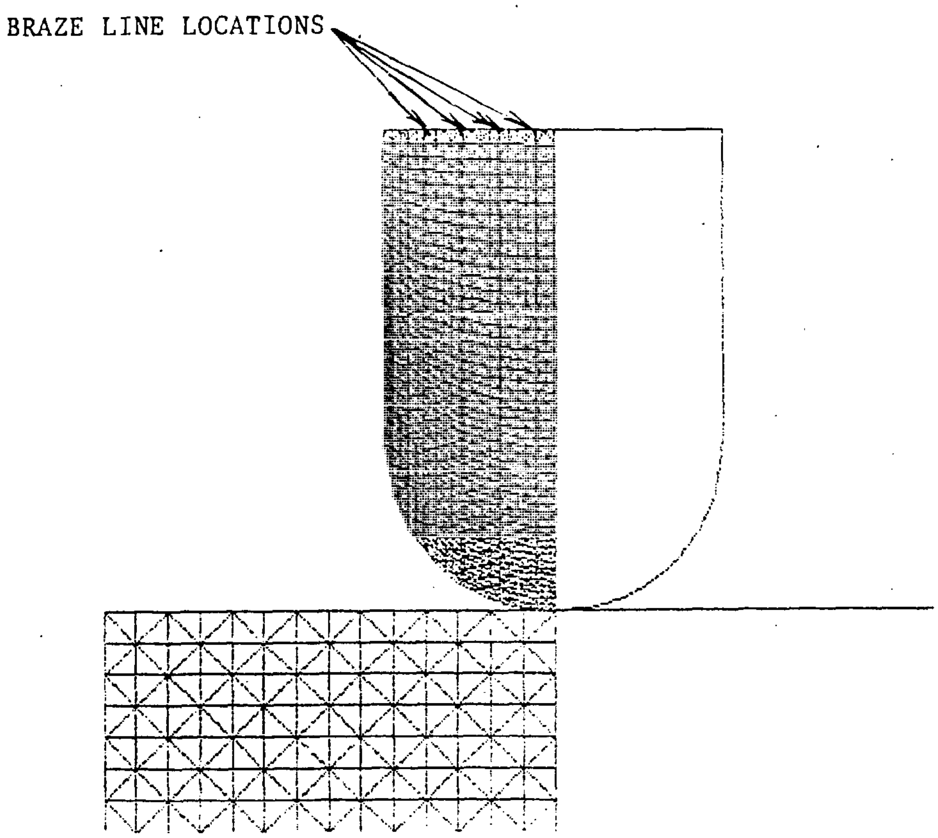

NINE LAYER PENETRATOR AT TIME t = 0
FIGURE 6A

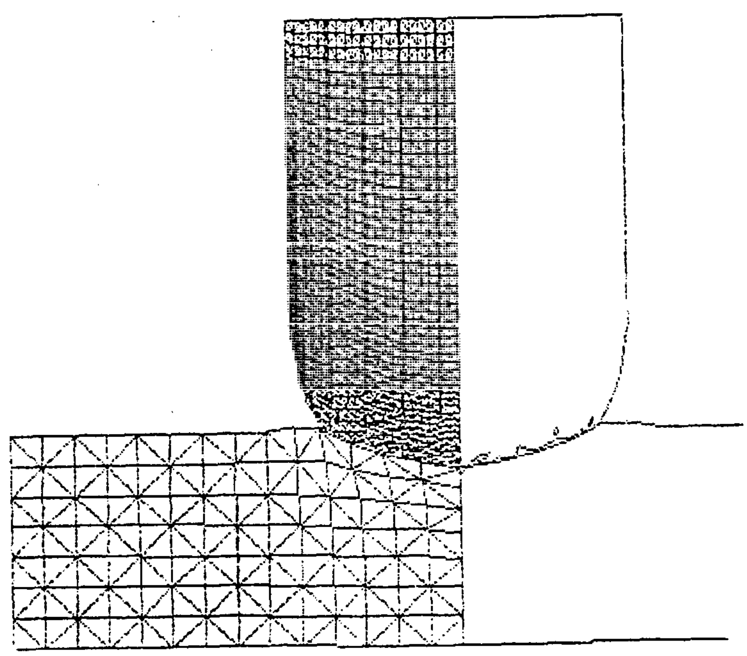

NINE LAYER PENETRATOR AT TIME t = 1 $\times 10^{-6}$
FIGURE 6B

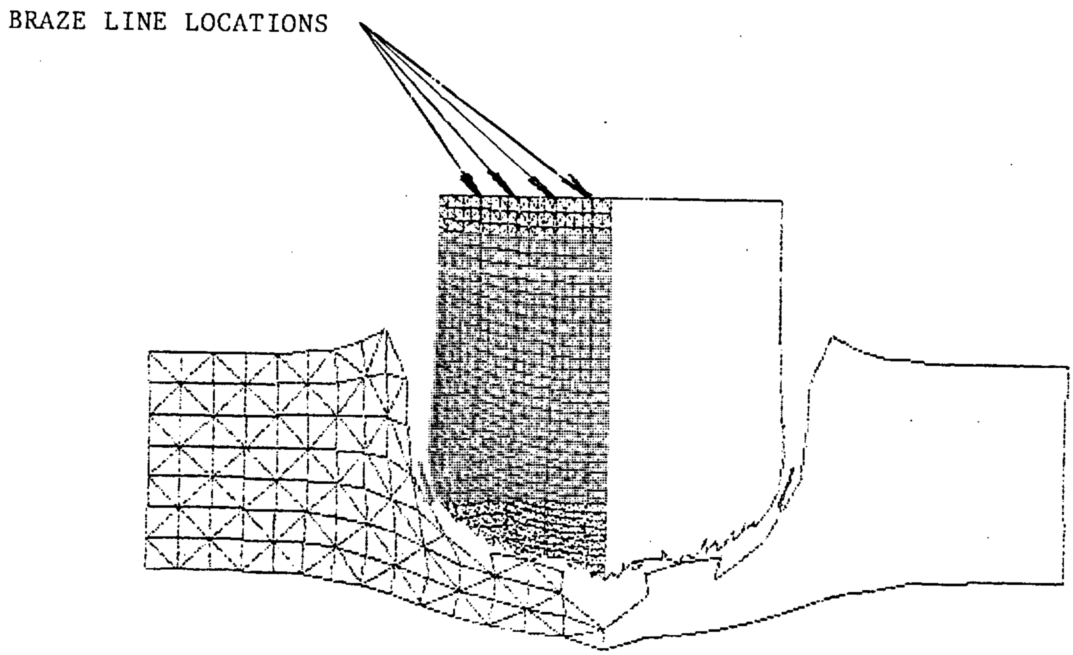

NINE LAYER PENETRATOR AT TIME t = 5 $x10^{-6}$
FIGURE 6C

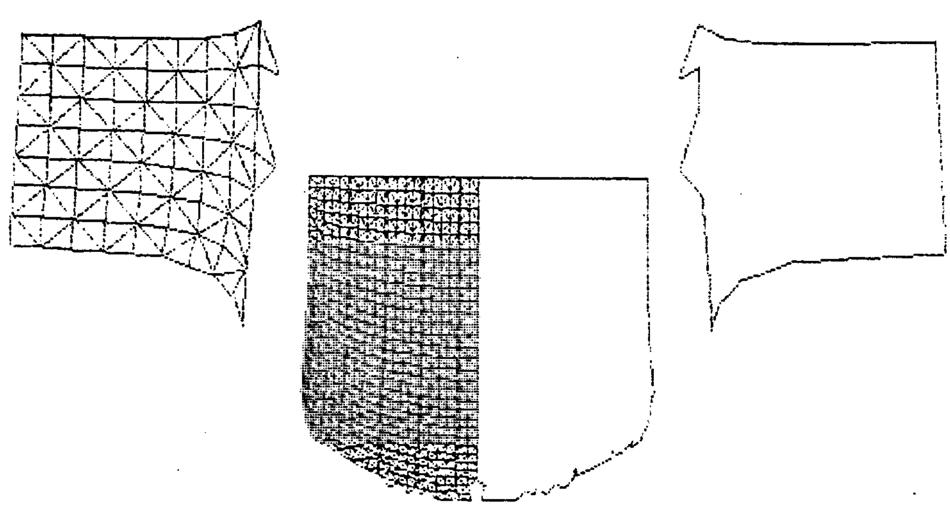

NINE LAYER PENETRATOR AT TIME t = 10 $x10^{-6}$
FIGURE 6D

The failure data selection input was then changed, however, the predictions still indicated no difference between the copper and nickel braze cases. This means that the failure data in the data base of the code is incorrect or the code is being improperly used.

The results for the six layer copper braze case is shown in Figure 7, and in Figure 8 for the nickel braze. The results for the nine layer copper case are shown in Figure 9. The results of the EPIC-2 code clearly indicate that there is a difference between the six and nine layer penetrators. It must be kept in mind that the code is analyzing an axisymmetric penetrator and not a two dimensional layered penetrator. The outer shells of the axisymmetric configuration may give more strength to the penetrator, since the outer layer or shell is less loaded and would prevent the penetrator from breaking up down the center. From the results of the predictions the nine layer penetrator is more effective at penetrating the target, but has a higher degree of break up along the centerline of the penetrator. The EPIC-2 calculations show that a 6 layer projectile penetrates faster than a 9 layer projectile but that it also breaks up faster. If the target was thicker, the fact that the 9 layer projectile does not break as fast may cause it to be more effective for thicker targets.

Another possible configuration may be a penetrator with outside layers that get progressively thicker towards the center of the penetrator. This type of configuration represents fine tuning of the concept. This type of fine tuning can be accomplished through the use of a code such as EPIC-2 or DYNA3D.

It was attempted to analyze a slide line or built in failure configuration with the EPIC-2 code. This code can not have different failure properties for a single node but only for a single line of grid points. Supposedly, the code DYNA3D has the capability of using different data for each grid point. The code DYNA3D is a better choice to use for any further work that is done in Phase 2. This code is available from Lawrence Livermore Laboratories. This code has been used on Silicon Graphics hardware and requires from 2 to 40 hours, depending on the complexity of the case being analyzed. Running the code on a more powerful machine, such as an SGI Crimson (which is a nominal 15 megaflop machine), will result in run times of about half an hour.

A final case tried with EPIC-2 was to use a weak set of failure properties along a line of nodes and compare this to a pure tungsten case. The results of these calculations are shown in Figures 10 and 11. The slide line projectile pierces the target at 10 x 10^{-6} seconds, whereas the pure tungsten projectile requires 12 x 10^{-6} seconds to pierce the target. The pure tungsten projectile indicates some slight degree of mushrooming at 5 x 10^{-6} seconds, but not to the extent that has been observed in experiments. At best the results of these calculations indicate that a layered slide line projectile appears to be better than a pure tungsten projectile.

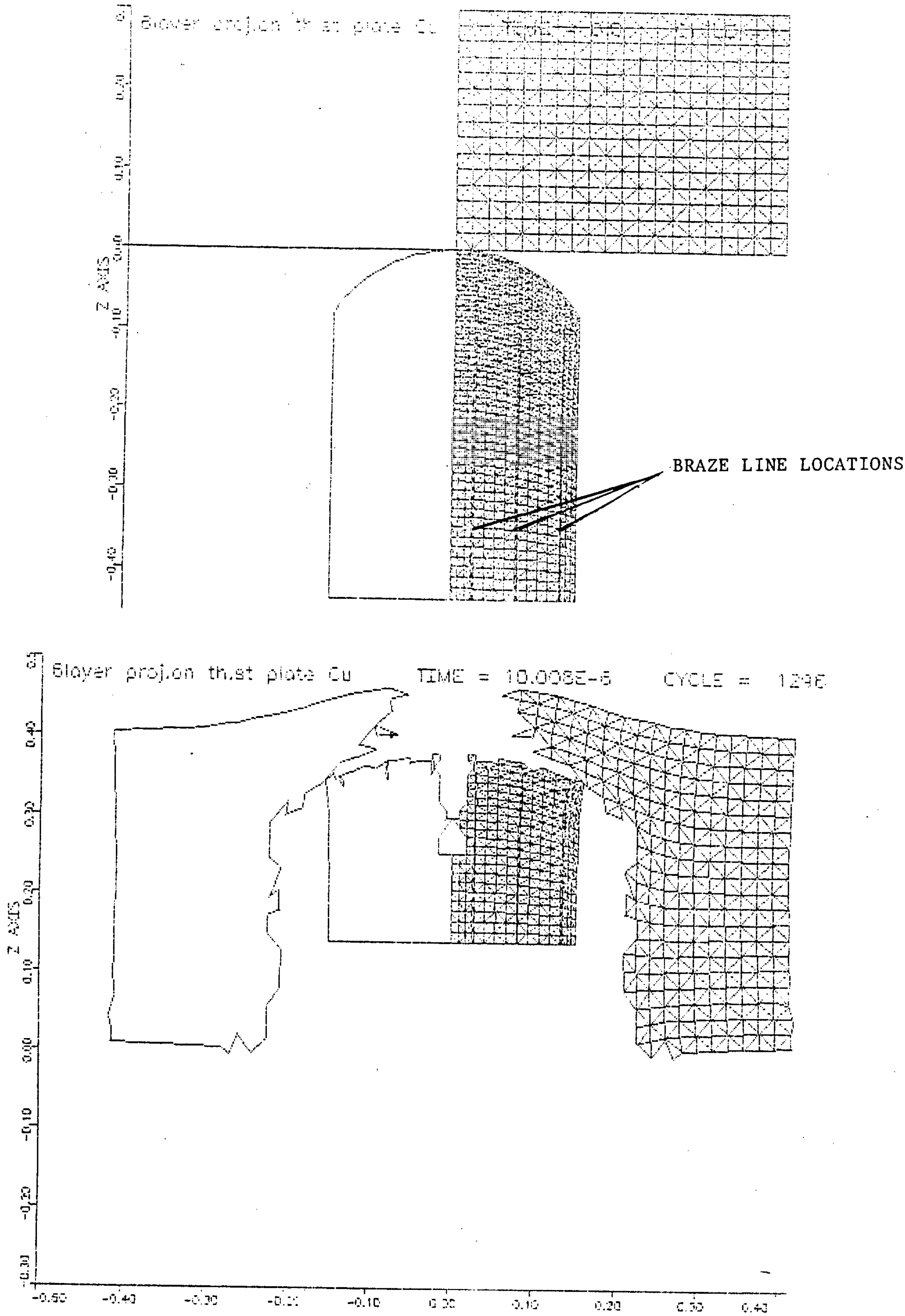

SIX LAYER COPPER BRAZE PENETRATOR RESULTS
FIGURE 7

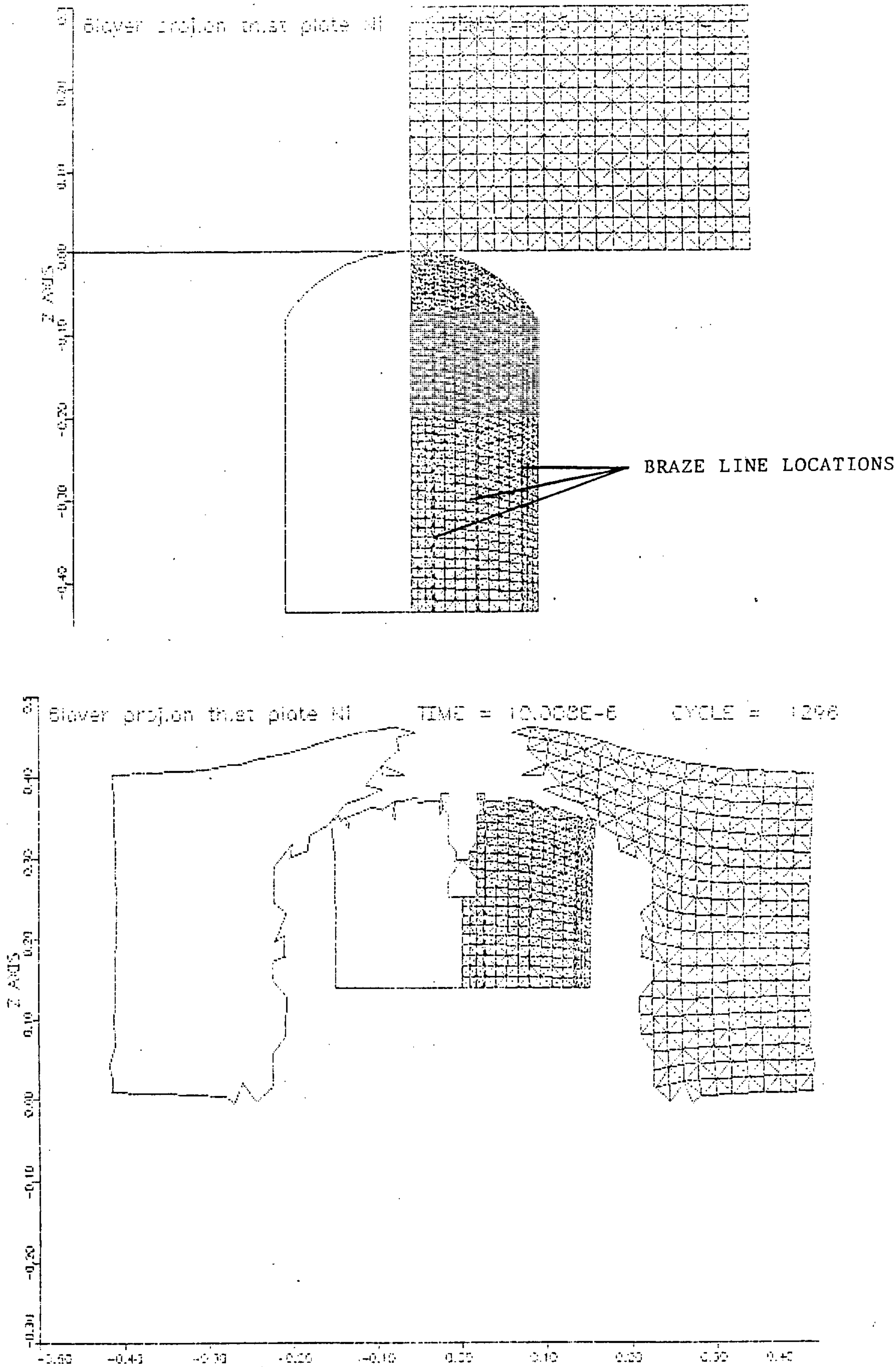

SIX LAYER NICKEL BRAZE PENETRATOR RESULTS
FIGURE 8

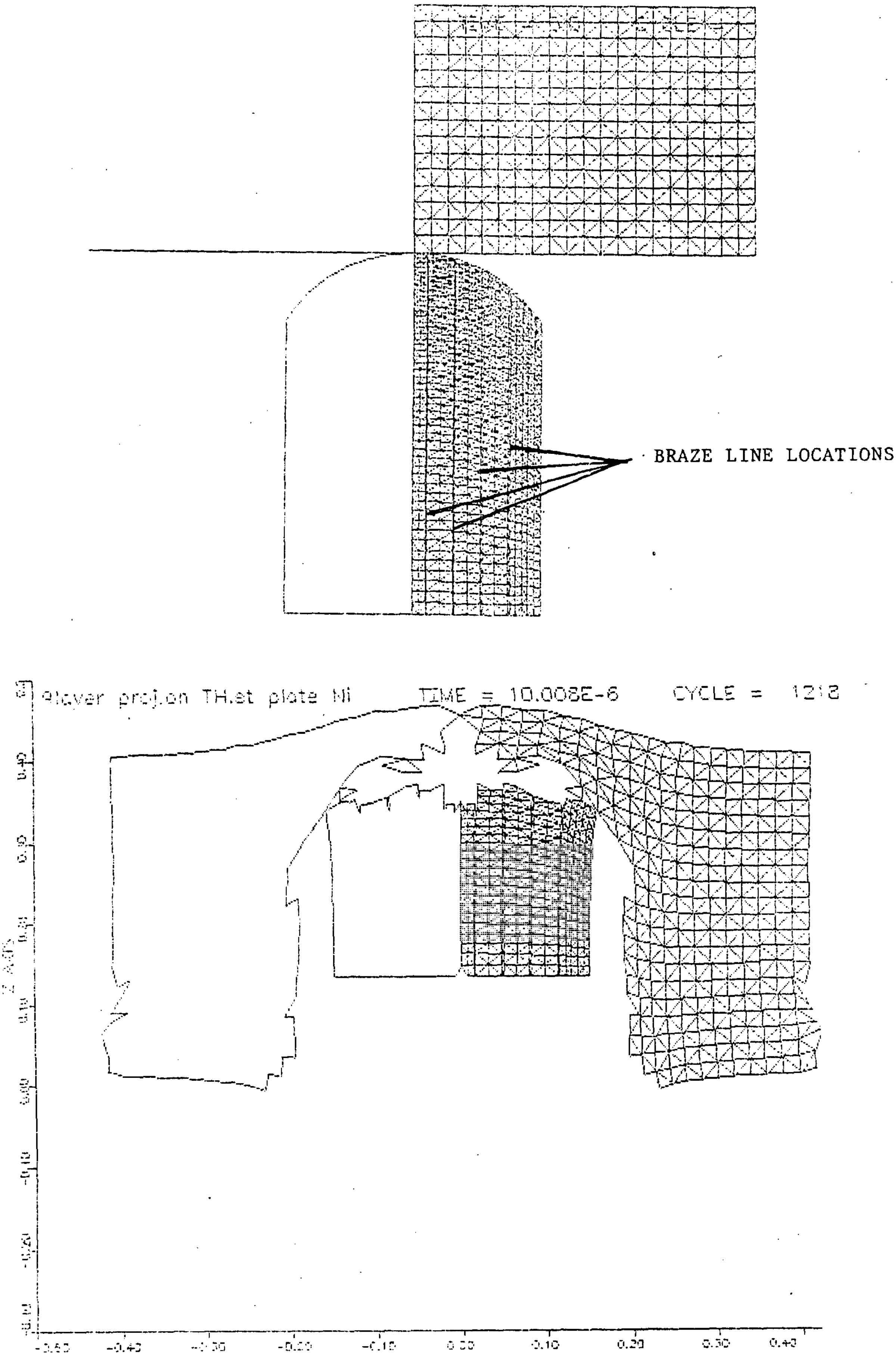

NINE LAYER COPPER PENETRATOR RESULTS
FIGURE 9

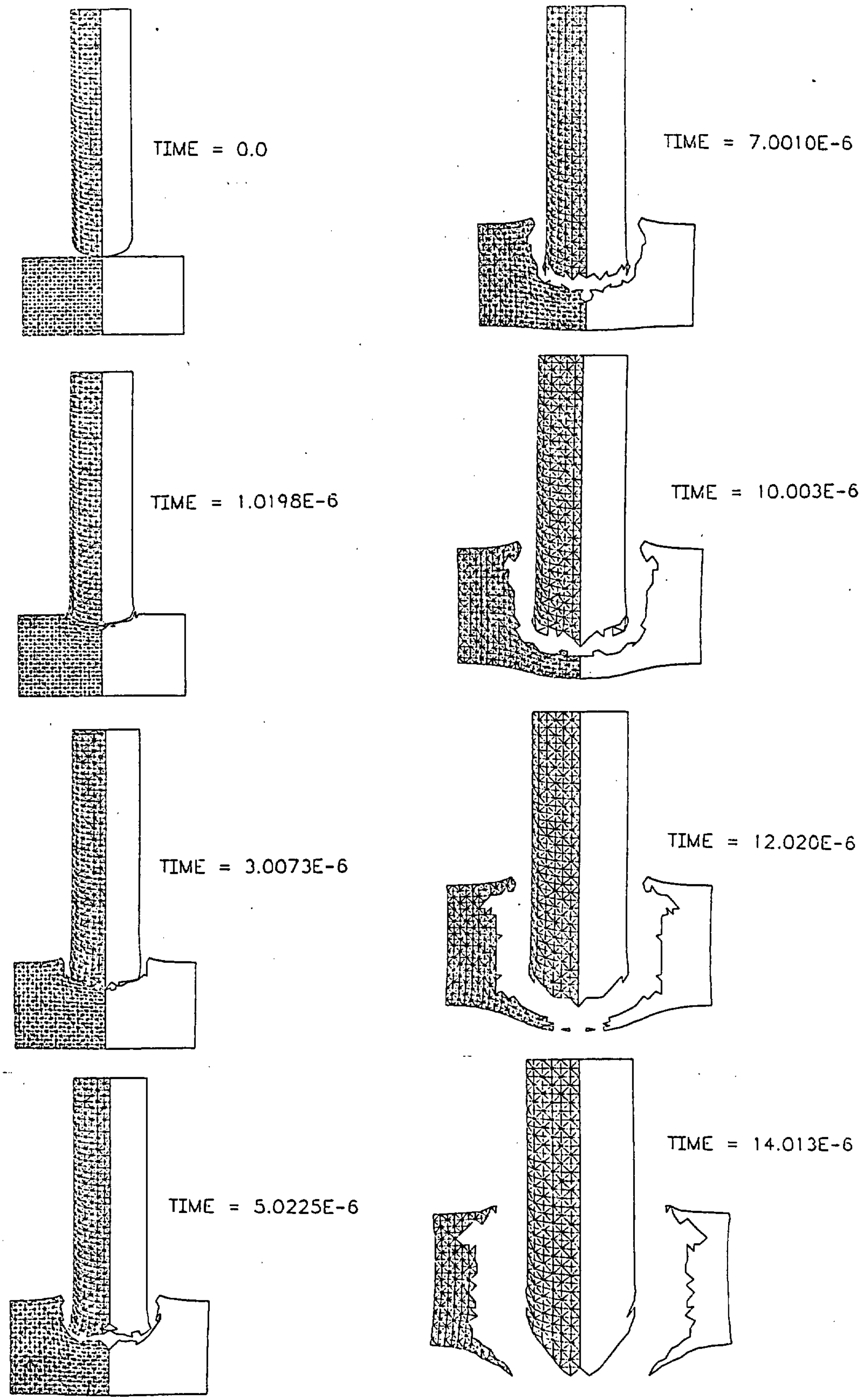

PURE TUNGSTEN PENETRATOR RESULTS
FIGURE 10

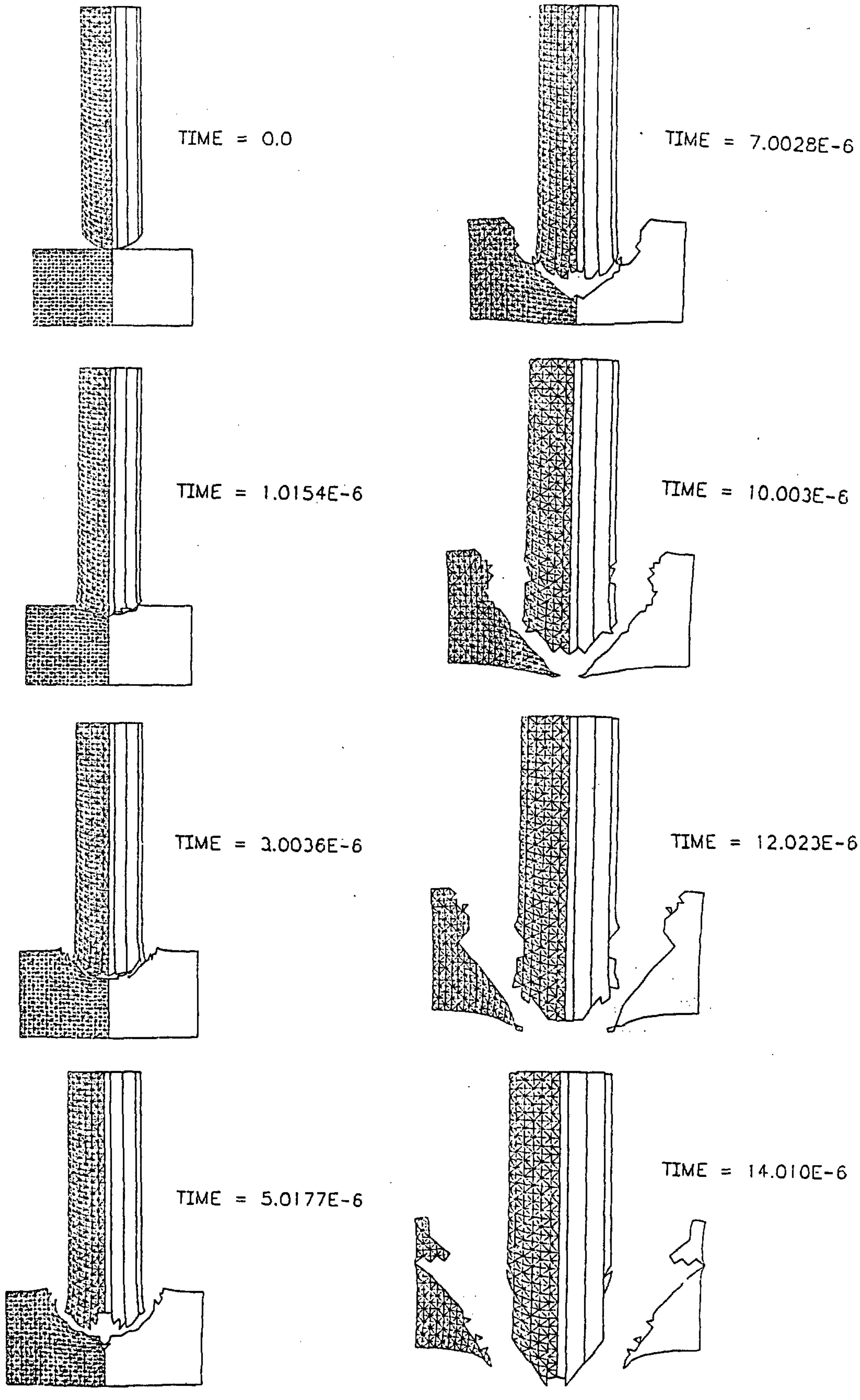

LAYERED SLIDE LINE PROJECTILE RESULTS
FIGURE 11

PENETRATOR FABRICATION

Two brazing materials were considered, OFHC copper and a nickel based brazing filler metal. The copper is typically 99% pure copper. The nickel brazing filler metal is Nicrobraz 135, obtained from the Wall Colmonoy Corporation in Madison Heights, Michigan. The properties of the Nicrobraz 135 are given in Table 1.

TABLE 1 NICROBRAZ 135 PROPERTIES

		Specifications AWS A5.8 AMS & others	Nominal Composition	Melting Point Solidus/Liquidus	Brazing Range (Suggested Brazing Temp)	Recommended Atmosphere	Oxidation Resistance Up Through	Joint Micro Hardness (Knoop)	Density lb/cu. in. (Specific Gravity)	For More Information See Nicrobraz Data Sheet No.
NICROBRAZ 135	Wide melting range, free-flowing properties, machinability, and low diffusion with most base metals.	BNi-4 4779 B50TF206	B 1.9 Si 3.5 C 0.06 max. Ni Bal.	1810 F / 1935 F 990 C / 1055 C	1950 - 2150 F (2050 F) 1065 - 1175 C (1120 C)	A,B	1800 F 980 C	150 to 400	0.303 (8.38)	2.1.17

This filler metal was selected based on a telephone conversation with technical representatives of the Wall Colmonoy Corporation. The discussion indicated that the strength of the braze joint using 135 can be varied by using different temperatures during the brazing process and holding the penetrator at the selected temperature for different periods of time. The higher the temperature and the longer the time, the more diffusion that occurs and thus the more homogeneous the resulting part. The hardness of the resulting joint is also a function of the brazing cycle. The more diffusion that occurs the lower the hardness of the resulting joint. Also mentioned was that there will be residual stresses that will occur in the brazed part. These stresses will be lower with the copper than with the nickel. This stress is related to the coefficient of expansion of the filler metal and the tungsten. The coefficient of thermal expansion of copper, nickel and the tungsten alloy are given below.

TABLE 2 - COEFFICIENT OF THERMAL EXPANSION

MATERIAL	COE*
COPPER	9.2×10^{-6}
NICKEL	7.4×10^{-6}
TUNGSTEN	2.5×10^{-6}

* PER DEGREE F

In selection of the penetrator configuration, the guidelines used were the following:

WEIGHT	65 GRAMS
DIAMETER (NOMINAL)	.30 INCHES
DENSITY	> 17.2 GM/CC
LENGTH (NOMINAL)	3.0 INCHES
L/D	10.0
VELOCITY	1500 METERS/SEC

In design of the test articles, two different tungsten alloy thicknesses were considered. The tungsten alloy used was HD 17D obtained from The Mi-Tech Corporation located in Indianapolis Indiana. The properties of this and other alloys that Mi-Tech makes are given in Table 3.

TABLE 3 MI-TECH TUNGSTEN ALLOY PROPERTIES

Mi·Tech® Material ▲	HD 17	HD 17 D	HD 17.5	HD 18	HD 18 D	HD 18.5
	90% W 6% NI 4% Cu	90% W 7% NI 3% FE	92.5% W 5.25% NI 2.25% FE	95% W 3.5% NI 1.5% Cu	95% W 3.5% NI 1.5% FE	97% W 2.1% NI .9% FE
Density Gms/cc	17	17	17.5	18	18	18.5
Density Lbs/cu. in.	.614	.614	.632	.650	.650	.668
Mil. Spec. T-21014 D	Class 1	Class 1	Class 2	Class 3	Class 3	Class 4
SAE Aero. Material Spec. (AMS) 7725B	7725B	7725B				
ASTM-B-459-67	Grade 1 Type II & III	Grade 1 Type II & III	Grade 2 Type II & III	Grade 3 Type II & III	Grade 3 Type II & III	Grade 4 Type II & III
Hardness Rockwell C	24	25	26	27	27	28
Ultimate Tensile Strength (PSI)	110,000	120,000	114,000	110,000	120,000	123,000
Yield Strength .2% offset (PSI)	80,000	88,000	84,000	85,000	90,000	85,000
Elongation (% in 1")	6	10	7	7	7	5
Proportional Elastic Limit (PSI)	45,000	52,000	46,000	45,000	44,000	45,000
Modulus of Elasticity (PSI)	40×10^6	45×10^6	47×10^6	45×10^6	50×10^6	53×10^6

A computer analysis was generated that determines the weight of a layered penetrator for different tungsten thickness, braze metal thickness and braze metal (either copper or nickel). Typical results of the computer code are shown in Table 4. For a selected penetrator radius, tungsten thickness, braze metal thickness and braze metal the penetrator length and weight are computed. The radius is then varied until the required weight of 65 grams is obtained. The results of this analysis gave the approximate dimensions for the fabricated penetrator.

TABLE 4 PENETRATOR CHARACTERISTICS

DESIRED PENETRATOR WEIGHT	=	0.143 POUNDS
DESIRED PENETRATOR WEIGHT	=	64.999 GRAMS
HEMISPHERE PENETRATOR WEIGHT	=	0.144 POUNDS
HEMISPHERE PENETRATOR WEIGHT	=	65.436 GRAMS
WEIGHT OF TUNGSTEN LAYERS	=	0.001 POUNDS
WEIGHT OF BRAZE METAL	=	0.012 POUNDS
DENSITY OF HEMI-CYLINDER PENETRATOR	=	0.603 LBM/IN**3
DENSITY OF HEMI-CYLINDER PENETRATOR	=	16.698 GM/CC
DENSITY OF CYLINDRICAL PENETRATOR	=	0.325 LBM/IN**3
DENSITY OF CYLINDRICAL PENETRATOR	=	9.000 GM/CC
DENSITY OF TUNGSTEN	=	19.300 GM/CC
DENSITY OF HD 17D	=	17.000 GM/CC
CYLINDER PROJECTILE LENGTH	=	5.690 INCHES
HEMI-CYLINDER PROJECTILE LENGTH	=	3.140 INCHES
RADIUS OF PENETRATOR	=	0.1570 IN
RADIUS OF 100% ALLOY	=	0.1557 IN
DIAMETER OF PENETRATOR	=	0.3140 IN
TUNGSTEN THICKNESS	=	0.0520 IN
BRAZE METAL THICKNESS	=	0.0020 IN

A preliminary fabrication evaluation was performed using purchased stock sizes of tungsten. The as received tungsten thickness was .25 inches thick, .40 inches wide and 12 inches long. The tungsten was machined to thicknesses of .025 and .050 inches and a length of 3.0 inches. These were then brazed using both copper and nickel brazing metal. A list of the brazed samples is given in Table 5. These were selected to determine the effect of braze metal, tungsten thickness and braze metal thickness.

TABLE 5 BRAZING TEST RUNS

PIECE	TUNGSTEN THICKNESS (INCHES)	BRAZE METAL	STOP OFF	WEIGHT (OZ.)
1	.050	CU	NO	57.4
1C	.050	NI	NO	57.4
2	.050	NI	NO	13.5
2C	.050	CU	YES	13.5
4	.025	NI	NO	15.0
4C	.025	CU	NO	15.0
5S	.050	NI	YES	15.0
5	.050	NI	NO	15.0

A weight was used to ensure that the tungsten stays in contact with the braze metal. The weight used is listed in the table.

The furnace chart showing the furnace temperature and pressure are given in Figure 12. The samples were clamped together and glued with super glue, the clamp was then removed. The glue was used to hold the sample together during handling prior to brazing. Two samples had 2 lines of Stop-off on one end. Stop-off is a generic name for chemical compounds that are used to prevent the flow of molten metal. It is basically a fine ceramic powder (the exact composition is considered to be proprietary by the manufacturer) suspended in a liquid base such as water or lacquer. There was one sample for copper and one for nickel braze metals. Thus one test sample performed two functions. One function was to see the effect of weight and the other was to see the effect of Stop-off. Each sample had 3 tungsten layers. Two samples had a nominal thickness .025 inches. The other samples had a nominal thickness of .050 inches. The samples were slightly bent due to the effect of the weight. The use of the nickel brazing transfer tape made it easy to assemble the test piece. The use of .005 inch copper stock required that the sample be clamped to assure that the sample was relatively flat. Use of .001 inch thick copper would result in less difficulty in assembling the test piece.

The Green Stop-off employed resulted in a black residue on the part after brazing. The only way to remove this is by sanding or grit blasting. A Red Stop-off can be removed with a 10% nitric or hydrochloric acid solution. The Green Stop-off is more effective than the Red Stop-off. This is because the Green Stop-off is a surface active material that froms a very thin oxide on the part, whereas the Red Stop-off is a parting compound and does not react with the surface to from an oxidized layer. This would require a thicker coating of Red Stop-off if it is used in place of the Green Stop-off. Depending on the tenacity of the brazing material, the Red Stop-off may not work. The brazing metal may flow under the Red Stop-off. Information from Wall Colmonoy indicates that a nickel based brazing material is more tenacious than copper.

Microscopic examination of the brazed test samples is shown in Figure 13a and 13 b and indicates that the copper results in a braze that had almost no voids. This was not the case with the nickel braze material. The nickel braze material employs an adhesive to fabricate the transfer tape. This adhesive may be the cause of the voids. As shown in Figure 13b, the braze layer is more uniform in the center of the braze than at the edges. This could be due to diffusion of the vaporized adhesive from the center to the edge. The thickness of the copper braze layer was estimated to be .0025 inches based on the photographs.

Twelve test penetrators were fabricated. Six of them were the same. The other six consisted of three groups of two different configurations. The 12 baseline penetrators had 7 layers of tungsten brazed with .005 inch copper foil. The tungsten was about .052 inches thick. Two penetrators were fabricated with nickel brazing material and two with lines of Stop-off where no brazing will occur. These lines were spaced a distance of .015 inches as shown in Figure 14. The final two penetrators had 13 tungsten layers where the tungsten thickness is .025 inches.

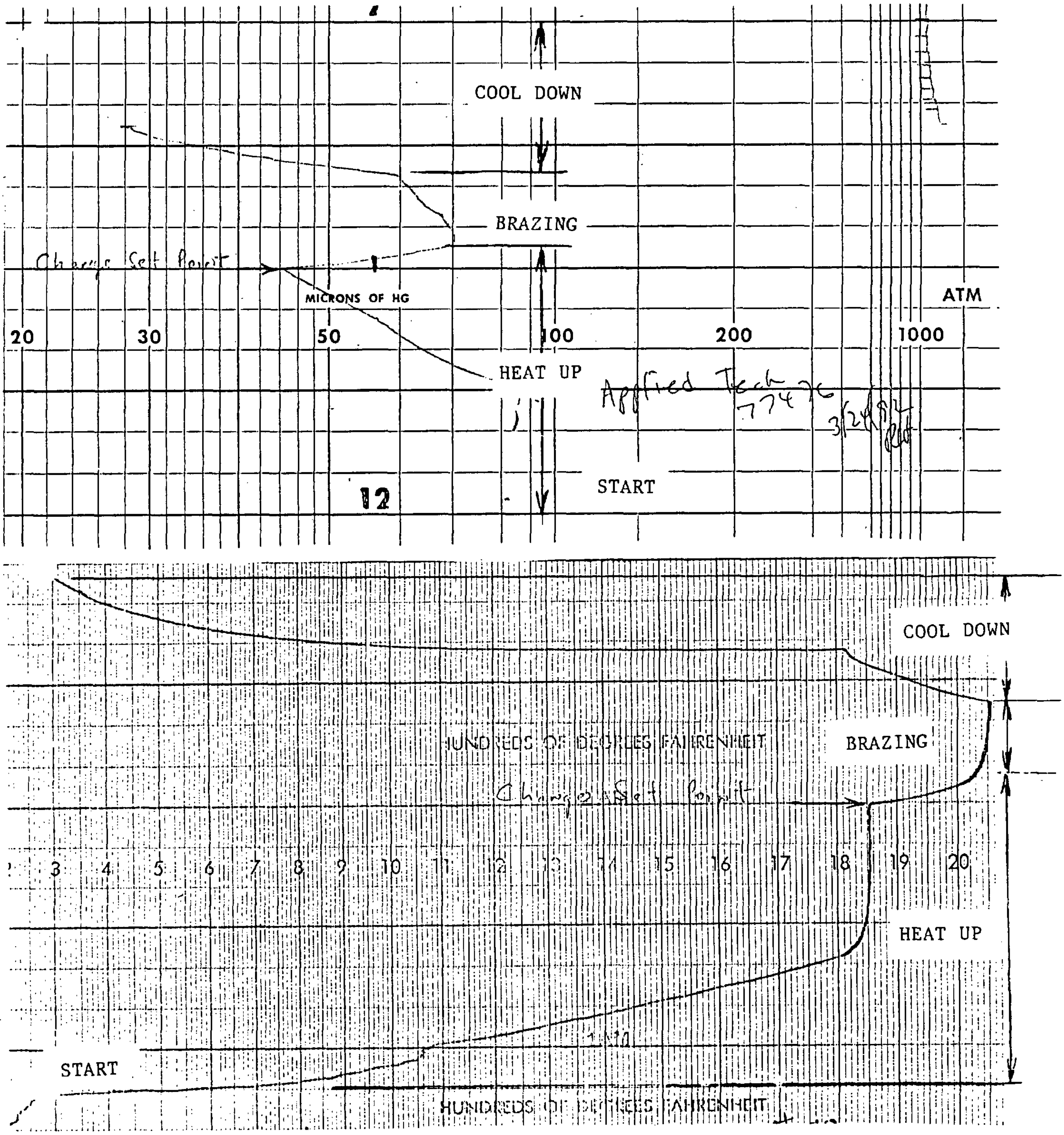

FURNACE TEMPERATURE AND PRESSURE
FIGURE 12

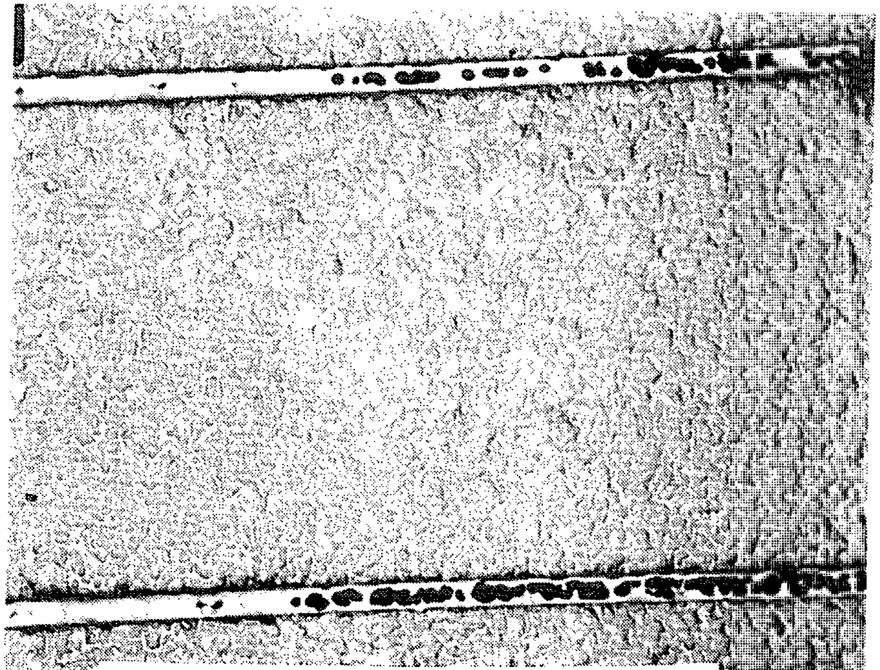

NICKEL BRAZE - 50 TIMES MAGNIFICATION

COPPER BRAZE - 50 TIMES MAGNIFICATION

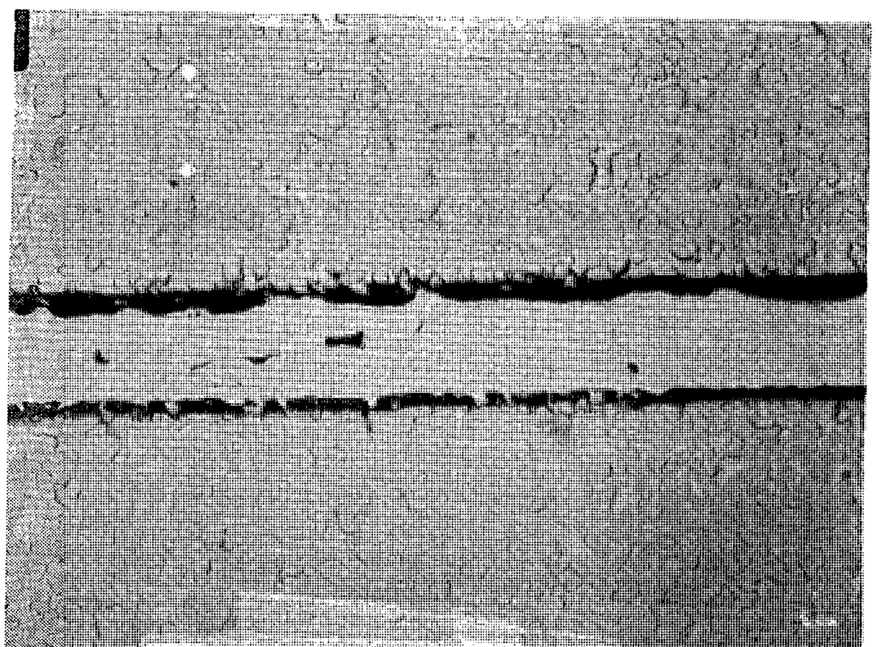

NICKEL BRAZE - 200 TIMES MAGNIFICATION

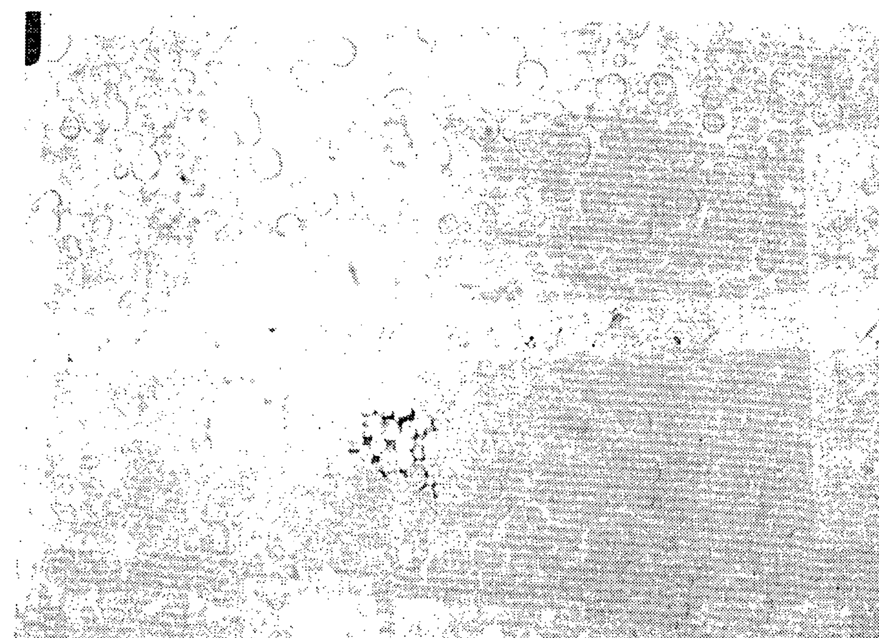

COPPER BRAZE - 200 TIMES MAGNIFICATION

BRAZE JOINTS
FIGURE 13a

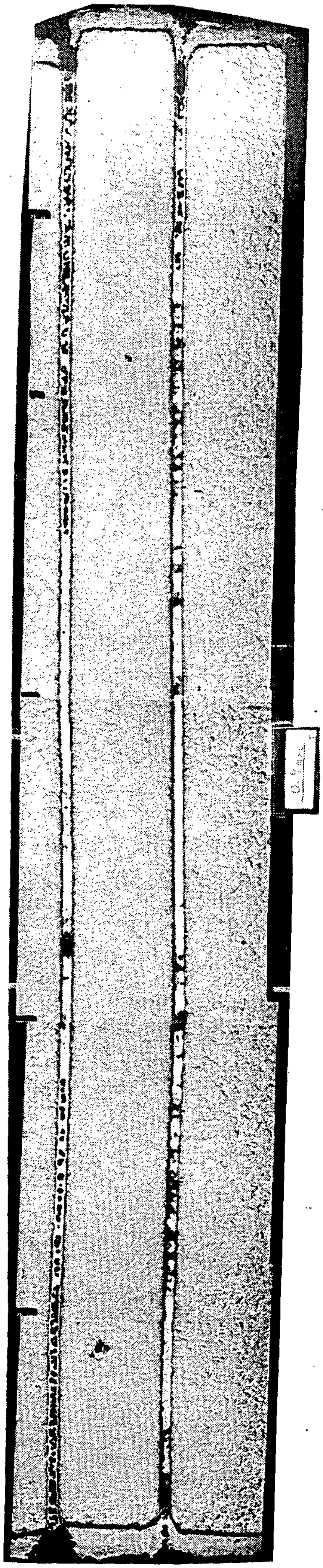

NICKEL BRAZE JOINT ACROSS ENTIRE WIDTH OF SAMPLE

BRAZE JOINTS
FIGURE 13b

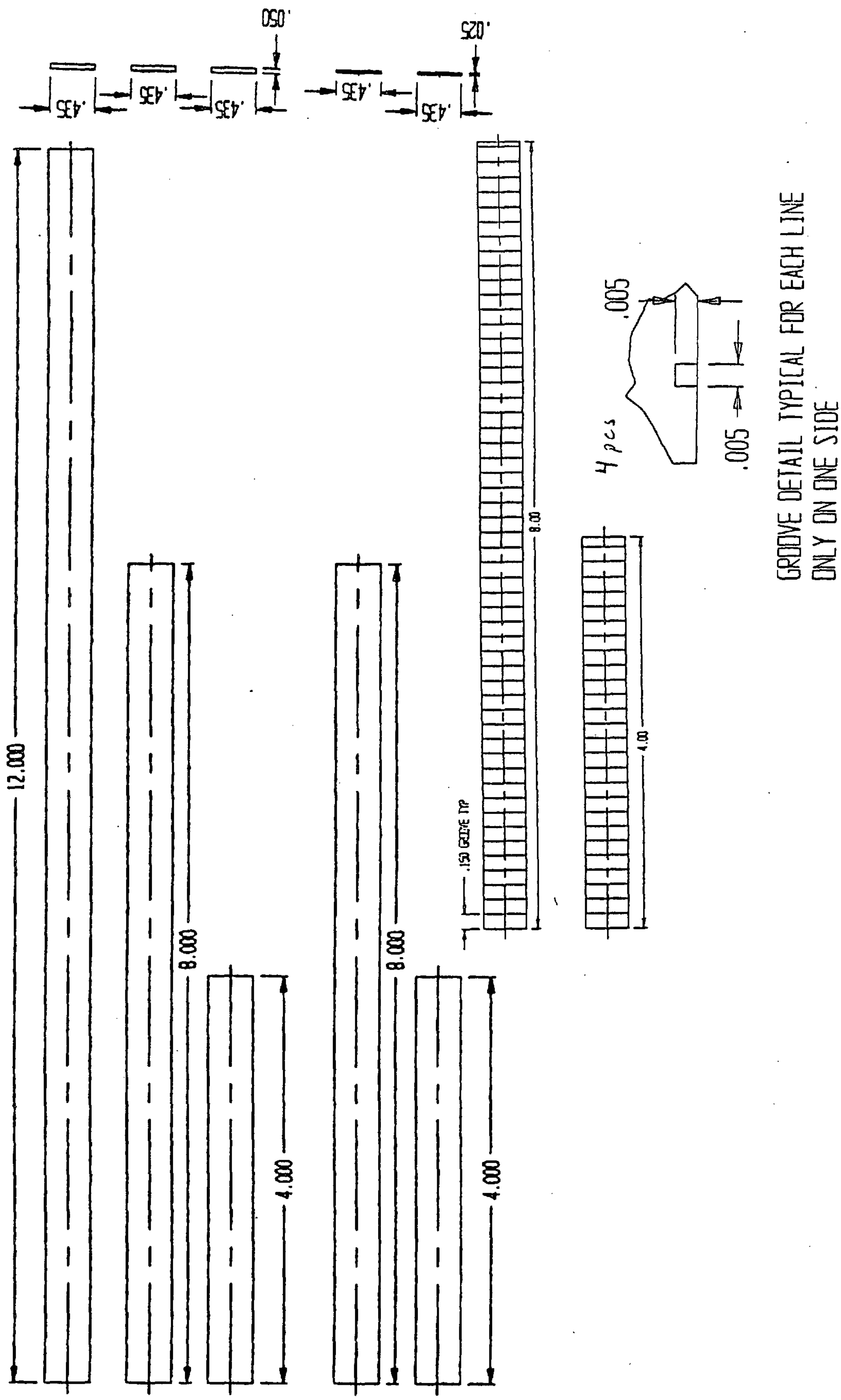

TUNGSTEN DIMENSIONS FOR TEST PENETRATORS PRIOR TO MACHINING
FIGURE 14

The initial width of the tungsten material was about .40 inches. This width was reduced to about .374 inches so that the sides of the tungsten were straight and they could be held in the fixture used to cut them to the required thickness.

During assembly of the 6 layer test sample with built in failure lines, stop off was used in the notches. The stop off was applied to the entire surface and allowed to dry. The surface was then sanded with emery paper (320 grade). After sanding, the stop off was still in the groves, but some additional stop off could be seen on the surface of the part in the tool marks. This means that a surface finish of 16 should be specified. This would prevent accumulation of residual stop off on the machined surface.

A brazing fixture was fabricated to hold the assembly flat during brazing. The fixture is illustrated in Figure 15. A nominal weight of 28 ounces was used on the short 8 inch pieces and a weight of 120 ounces on the 12 inch long pieces. The weight did not extend the entire length of the tungsten. There was a one inch section on each end that had no weight. It was believed that when the copper melts the tungsten would squeeze the copper down to a uniform thickness. This did not happen. Measurements were taken on each piece. The results of these measurement are shown in Figure 16. The initial thickness of the tungsten was .052 and .026 inches thick. For the 7 layer piece this gives a tungsten thickness of .364 inches and for the 13 layer piece, this gives a tungsten thickness of .325 inches. Using the measured thickness values, the nominal braze thickness was .0018 to .0023 inches for the .052 inch thick pieces and .0031 to .0043 inches for the .026 inch thick pieces. These values indicate that a weight should be applied to the entire length of the pieces being brazed.

Visual inspection of the brazed parts indicate the nickel did not flow as much as the copper. This can be seen in Figure 17. Also shown are the brazed pieces with the thin layers (.026 inch thick) and the notches. The notched piece shows small holes where the stop off was located.

A sensitivity study was done to determine the effect of diameter on penetrator weight. The results of this are given in Table 6. For a diameter variation of .314 to .316 inches the weight varies from 65.436 to 66.67 grams. This is with a braze layer thickness of .002 inches. If the braze layer thickness is varied from .0020 to .0035 inches, the weight varies from 65.436 to 64.790 grams. For the .026 inch thick layers, as the diameter varies from .314 to .316 inches the weight varies from 65.808 to 67.111 grams, this is with a braze layer thickness of .0020 inches. Keeping the diameter constant at .314 inches and varying the thickness of the braze layer from .002 to .003 inches changes the weight from 65.808 to 63.998 grams, respectively. Thus a diameter of .314 inches and a .0025 inch braze layer appear to be nominal values to obtain a 65 gram projectile. Tolerances on the diameter are on the order of .001 inches.

TABLE 6 EFFECT OF DIAMETER AND BRAZE THICKNESS ON WEIGHT

LAYERS	DIAMETER (INCHES)	LENGTH (INCHES)	WEIGHT (GRAMS)	BRAZE THICKNESS (INCHES)
7	.314	3.14	65.436	.0020
7	.314	3.15	66.052	.0020
7	.314	3.16	66.670	.0020
7	.314	3.14	65.222	.0025
7	.314	3.14	65.007	.0030
7	.314	3.14	64.790	.0035
13	.314	3.14	65.808	.0020
13	.315	3.14	66.460	.0020
13	.316	3.14	67.111	.0020
13	.314	3.14	65.105	.0025
13	.314	3.14	63.998	.0030

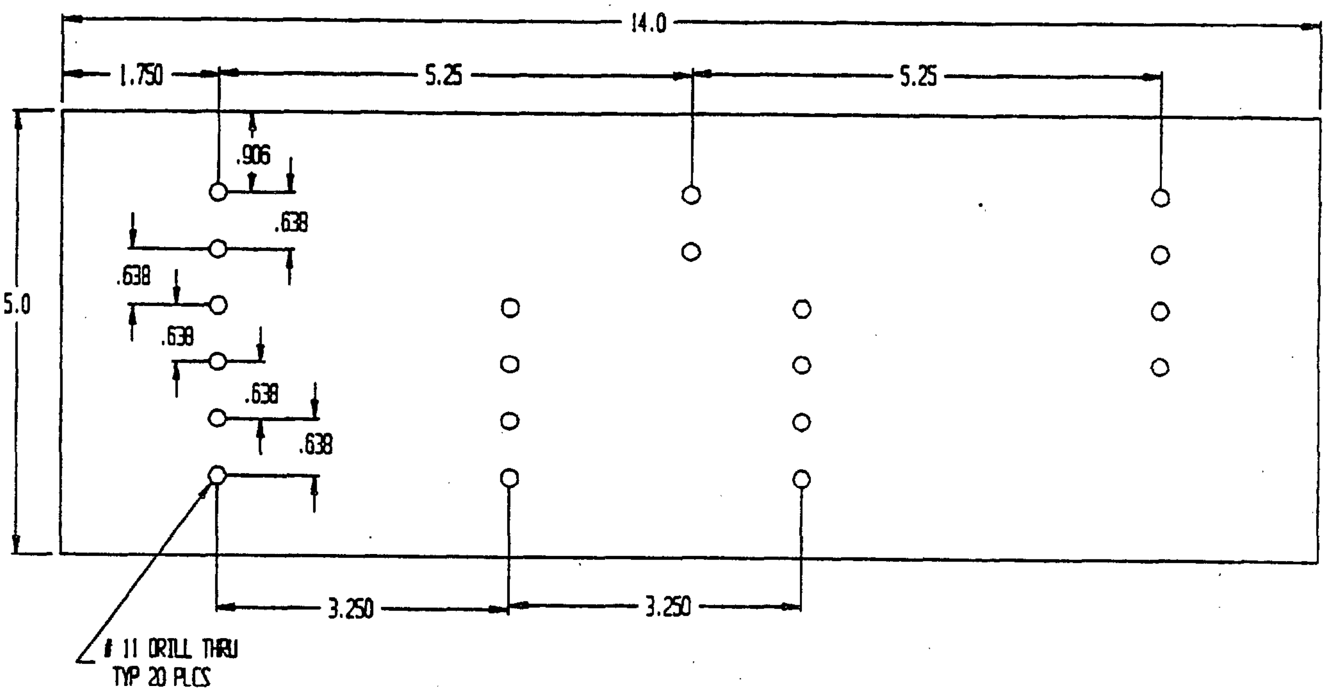

BRAZING FIXTURE
FIGURE 15

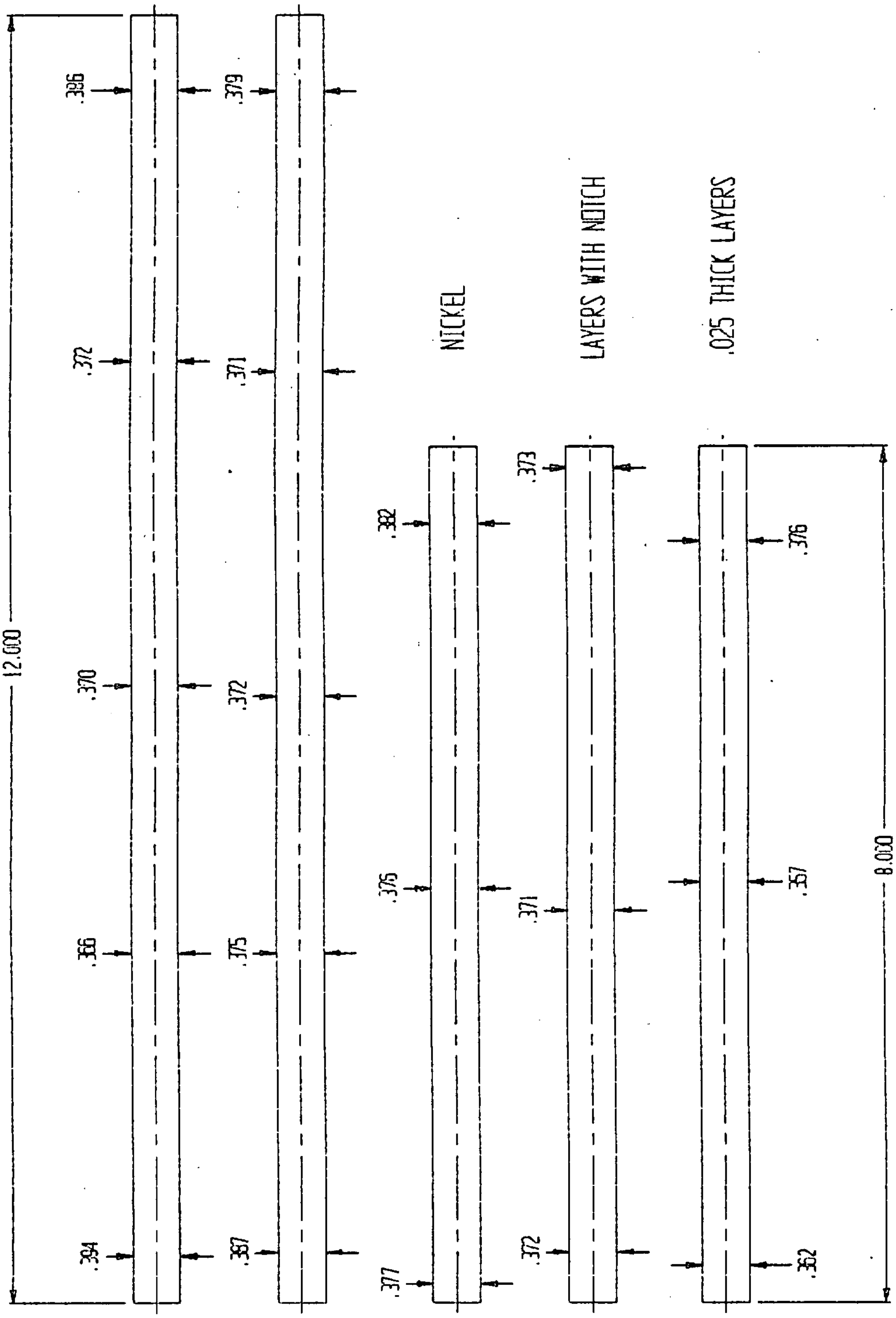

DIMENSIONS OF BRAZED PART PRIOR TO MACHINING
FIGURE 16

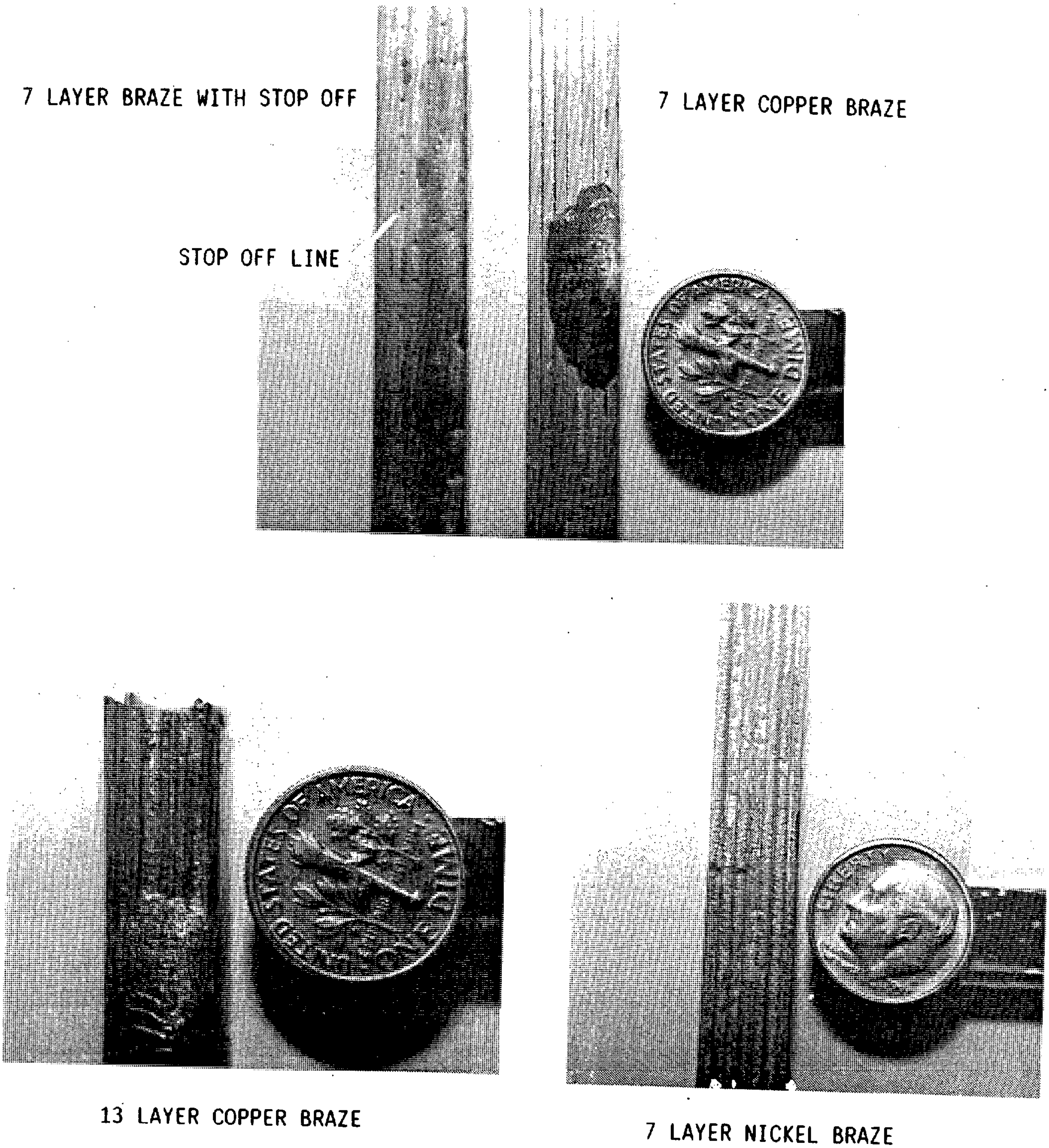

PHOTOGRAPHS OF BRAZED LAYERS
FIGURE 17

A test braze was also done using two stacked layers of .005 inch thick copper and two tungsten pieces. The pieces were separated by .010 tungsten wire. The purpose was to see if the copper would run out from between the pieces. The results of the braze showed that the copper did not run out. This means that using a spacer of up to .010 inches, a thicker braze can be obtained. This may also be a method to guarantee better control over the thickness of the braze.

The fact that there was bending of the parts during the machining and the final brazed parts were not flat results in a nonsymmetrical penetrator. Typically there was .032 to .038 warpage (from the end to the center) of the 12 inch long pieces and .011 to .015 inches for the 8 inch long pieces.

The procedure used to machine the penetrator to the final dimensions and weight consisted of the following steps.

1. The brazed pieces were cut to 4 inch lengths.
2. A short length (.50 inches) of one end was rounded off in a lathe.
3. The piece was flipped over and held by the rounded end.
4. A center was machined into the other end and held by the lathe spindle.
5. The part was turned to the required diameter.
6. The length was cut to .010 inches oversize.
7. The hemisphere nose was machined.
8. The part was weighed.
9. The weight was ratioed to the required weight of 65 grams.
10. The weight ratio was used to determine the final length required.

The weight of the material in the nose of the 7 and 13 layer projectiles was 1.1 to 1.2 grams.

Before the parts were machined to their final shape, they were cut to a 4 inch length with a hacksaw. The nickel brazed part could not be cut with a hacksaw but had to be cut with a Carborundum disk. Although the nickel part was harder to cut, there did not seem to be any difference in machining to the final dimensions.

In the process of turning the parts on the lathe, it appears that the tungsten was tearing in the vicinity of the braze joint. This is evident by the approximately .001 inch voids that can be seen on the projectile. A photograph of this is presented in Figure 18. One of the projectiles, number 3 was machined to .0005 oversize and then polished to its final dimension with emery paper. This sample does not exhibit the same number of voids at the braze joint as the other ones do. The dimensions and weights of the test penetrators are given in Table 7 and photographs are presented in Figure 18. Due to an error in the computer code that determines the projectile weight, penetrator number one is under weight. The error in the computer code was due to using the wrong thickness for the outermost layer. The error effected the thick layer projectile and had a small effect on the thin layer projectile.

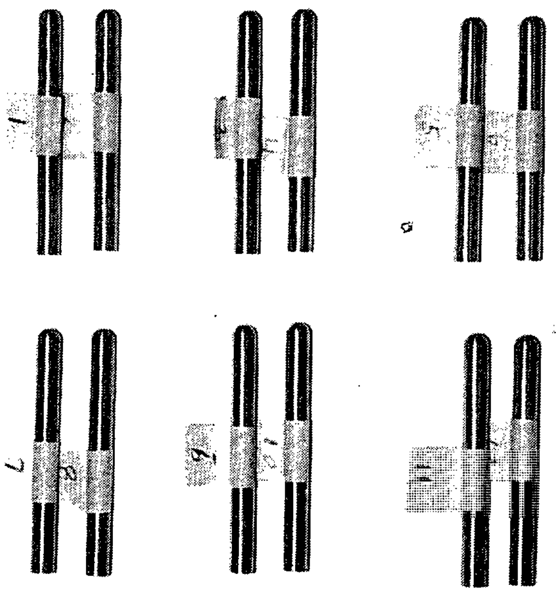

PENETRATORS 1 THROUGH 12

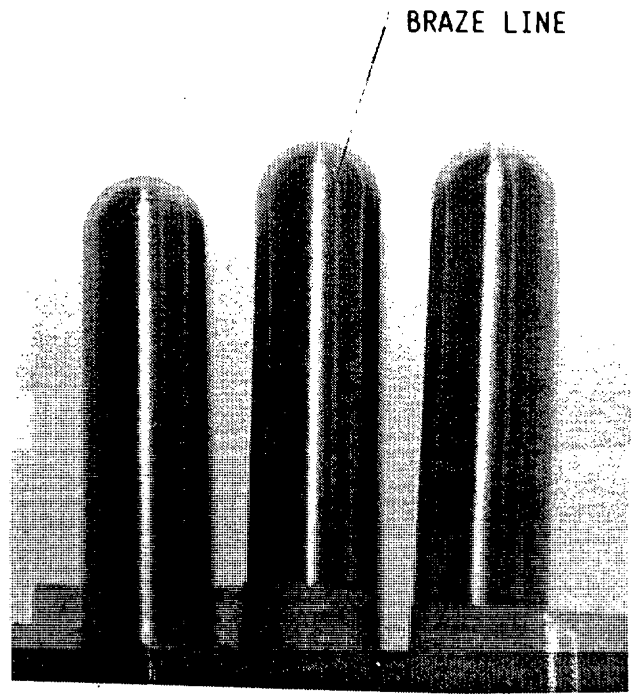

PENETRATORS 1 THROUGH 3

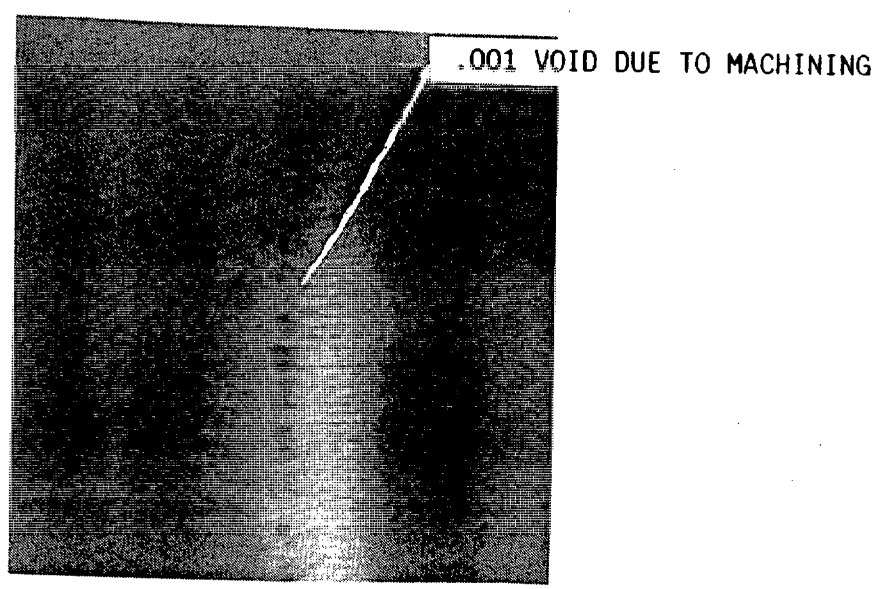

PHOTOGRAPHS OF TEST PENETRATORS
FIGURE 18

TABLE 7 DIMENSIONS AND WEIGHTS OF PROJECTILE TEST SAMPLES

NUMBER	DESCRIPTION	DIA IN.	LENGTH IN.	L/D	L/D %ERROR	WEIGHT GM	WEIGHT %ERROR	DENSITY GM/CC
1	.052,CU	.307	3.210	10.456	4.60	63.10	2.92	--
2	.052,CU	.314	3.140	10.000	0.00	64.90	0.15	16.69
3	.052,CU	.314	3.140	10.013	0.13	65.00	0.00	16.69
4	.052,CU	.314	3.134	9.981	0.19	65.00	0.00	16.69
5	.052,CU	.314	3.129	9.965	0.35	65.10	0.15	16.69
6	.052,CU	.314	3.121	9.939	0.61	65.05	0.07	16.69
7	.052,CU,V	.314	3.118	9.930	0.70	65.00	0.00	16.69
8	.052,CU,V	.314	3.140	10.000	0.00	65.00	0.00	16.69
9	.052,NI	.314	3.144	10.013	0.13	64.92	0.12	16.69
10	.052,NI	.314	3.151	10.035	0.35	65.00	0.00	16.69
11	.026,CU	.315	3.190	10.127	1.27	65.20	0.31	16.79
12	.026,CU	.316	3.150	9.968	0.32	65.10	0.15	16.80

PENETRATOR TESTING

The testing of the above penetrators was performed at the Army Materials Technology Laboratory in Watertown Massachusetts. The first 5 test articles were depth of penetration tests. Test articles 6,7 and 8 were A frame tests and the last 4 test articles were depth of penetration tests.

The flash photography from test article number 6 indicated that there was quite a bit of break up after the penetrator emerged from the first plate. This test also showed some flaring at the base of the penetrator. It was not possible to recover any of the fragments from the witness boxes for this test. The flash photographs from test article number 7 indicated a much lower degree of break up of the penetrator. Test pieces recovered from the witness boxes indicated that at least some of the break up occurred either on the braze lines or the transverse lines where the Stop-off was used in the v notches.

The depth of penetration tests indicated that the thick layer (.050 inches) performed poorer than a baseline tungsten alloy. A complete summary of the test results is presented in Appendix A. The base line alloy used for comparison was 91% tungsten which has a density of 17.2 gm/cc. In general the thin layer penetrator performed at about the same level as the base line alloy penetrator. The nickel brazed penetrator seemed to perform better than the copper braze penetrator.

The results of these tests imply that in general a layered tungsten penetrator does have merit and by optimizing the braze material, orientation of the braze lines and the penetrator assembly, performance at least equal to that of a standard tungsten alloy penetrator is possible. The tests also imply that a penetrator composed of many thin layers performs better than one composed of fewer thick layers. This may be due to the fact that each layer interface represents a potential shear line. To circumvent the problem of lower overall density due to the presence of the braze layer when a large numbers of tungsten layers are employed, a thin plated coating of copper or nickel can be used. Previous brazing tests performed in reference 2 indicated that the minimum copper thickness required for a strong braze joint was between .0003 and .0005 inches thick.

A copper thickness of .0002 inches was not sufficient. Further work on layered configuration where a solid tungsten alloy substrate is used to attach the outer tungsten layers, may offer performance better than that of a standard solid alloy penetrator.

CONCLUSIONS

A layered tungsten alloy kinetic energy penetrator that has built in failure lines showed that it has comparable depth of penetration performance to a homogeneous tungsten alloy penetrator. In A frame tests the penetrator exhibited more break up than a homogeneous penetrator due to bending failure along the "failure lines" (braze joints). A penetrator that consists of a large number of thin layers performed better than the same size penetrator that had a fewer number of thicker layers. Test results indicated that further reduction in layer thickness should improve penetrator performance. Also the nickel braze material appeared to perform better than the copper. The combination of these two effects could result in a penetrator that is superior to a baseline tungsten alloy penetrator. Further analytical work in conjunction with experimental testing should be performed to achieve an optimized layered penetrator configuration.

REFERENCES

1. Johnson, G.R., and Stryk, R.A., User Instructions for the EPIC-2 Code", AFATL-TR-86-51, September 1986.

2. Cavalleri, R.J., "Transpiration Cooling Nose Tip Technology", BMO TR-90-41. March 31, 1990.

3. Cavalleri, R.J., "Transpiration Cooling Nose Tip Technology", User's Manual, BMO TR-90-65. April 23, 1990.

4. Brazing Manual Table A1, p 44, American Welding Society, Third Edition

5. Wigley, D.A., "Technology for Pressure-Instrumented Thin Airfoils Models, NASA CR 3891, September 1985.

6. Wigley, D.A., "Technology for Pressure-Instrumented Thin Airfoils Models, NASA CR 4173, September 1988.

7. Wigley, D.A., "The Structure and Properties of Diffusion Assisted Bonded Joints in 17-4 PH, Type 347, 15-5 PH and Nitronic 40 Stainless Steels", NASA CR 165745, July 1981.

APPENDIX A

ARMY MATERIALS TECHNOLOGY LABORATORY TEST RESULTS

DEPARTMENT OF THE ARMY
U.S. ARMY LABORATORY COMMAND
MATERIALS TECHNOLOGY LABORATORY
WATERTOWN, MASSACHUSETTS 02172-0001

REPLY TO
ATTENTION OF

SLCMT-MRD (P. Woolsey) 27 August 1992

Dr. Robert Cavalleri
Applied Technology Associates, Inc.
P.O. Box 149434
Orlando, FL 32814

Subject: Ballistic Test Results for Laminated WHA Penetrators

Dear Robert :

Ballistic testing of the laminated tungsten alloy penetrators which you produced under the Phase I SBIR contract has been completed. A summary and analysis of the test data is provided herein for your information.

The standard penetrator used for comparison purposes is a 91% WHA (X-27C) from Teledyne Firth Sterling; it has a Ni-Fe binder, and is in the 25% swaged & aged condition. Its mass is 65 g and its aspect ratio is 10:1, the same as the supplied penetrators. The conditions of constant mass (i.e. constant energy) and L/D provide a means to readily examine the penetration performance of alloys with differing densities. An extensive dataset for penetration performance as a function of velocity is available, together with A-frame target results, and post-mortem analyses.

All of the supplied penetrators were fired at either a semi-infinite RHA steel block, to allow determination of penetration efficiency, or at an "A-frame" oblique plate target to provide a qualitative estimate of the penetrator resistance to bending failures. The RHA steel plate is 5" thick and has properties per MIL-P-12560G (Class 3); its hardness is approximately 28 Rockwell "C". The A-frame target is made up of a dual-plate initial element consisting of 2 plates of High Hardness Steel (MIL-P-46100, about HRC 52), each 0.25" thick, at an obliquity of 45°; this is followed by a single plate element of RHA steel, 0.625" thick (HRC ~32), at an obliquity of 30° reverse. This configuration is intended to increase the severity of the test by reversing the sense of the bending moment applied to the rod by the second target element from that imparted by the first element.

The semi-infinite penetration results were quite interesting. The shot results are summarized in Table 1, and the data are presented graphically in Figures 1 and 2. Out of the complete series, only the initial round was lost due to poor yaw (penetrator #1). As this was the low mass rod, its lack is not overly significant. Note that a linear fit for obtaining residual penetration with the baseline penetrator is shown on the plot in Figure 1; this will allow the average performance of the standard rod to be determined at any striking velocity within the range shown on the plot. Only representative baseline points are shown for the sake of clarity. The 7 layer laminate with Cu braze was the poorest performer.It is still close to the baseline, but appears to be dropping off as the velocity increases. The 7 layer Ni brazed penetrators and the 14 layer Cu brazed rods appear to be roughly equivalent for the limited number of tests performed with each (2 shots). Each of these also approximates the baseline alloy performance. It is interesting to note that the 14 layer structure outperformed the 7 layer structure. Please be aware the quantitative differences between these tests are not particularly large, and that these descriptions are based upon my subjective judgement of the tests, which includes the trends observed with other WHA materials as well as the nature of the penetration cavities.

Appearance of the penetration cavity varied between each of the laminate structures tested. The 7 layer Cu penetrators left a heavily scalloped cavity, which bears some resemblance to that created by a segmented rod, or by a normal penetrator in high hardness steel, in that there are distinct necks or variations in diameter over the length of the cavity. The 7 layer Ni exhibited this phenomenon also, although to a lesser degree. The 14 layer Cu penetration cavities appeared substantially more like the baseline alloy, although the tip tended to be more pronounced. In contrast to the above observations, average penetration cavity diameters did not vary beyond the normal bounds of observed results. Specimens of the residual penetrators will be taken and polished for micrographic observation of the failure modes as time permits.

The only penetrator configuration tested with the oblique plate A-frame target was the 7 layer Cu design. The shot results for these, together with two tests using the reference alloy, are summarized in Table 2. The residual rod length (defined as the longest section or continuous group of sections of penetrator observed behind the second target element on the X-ray film) is about the same for both cases. Residual velocities, however, are definitely higher for the baseline alloy. The laminated penetrator also exhibited a significant amount of both transverse and longitudinal fracture, which is usually evident on the film, and is definitely evident in the recovered penetrator fragments. The residual penetrators of baseline alloy were recovered essentially intact from the soft-catch packages, while the laminated rods had separated into a fairly large number of fragments. Some of these were of substantial size, and retained a fair penetrative capability. There is a tendency toward either complete transverse fracture or stair-step fracture (some transverse fracture followed by interlaminar separation) in the laminate design tested. Since all three penetrators failed in a similar fashion, I would not suspect the V-notches in the last two rods of having a significant effect on their behavior. There is a possibility that the degree of mushrooming may be slightly lower in the laminated penetrators, but this cannot be quantified due to the fragmentary nature of the recovered specimens. Complete longitudinal failure does not seem to have occurred; this is a promising point. An examination of the fracture surfaces is planned and will be done this fall.

It appears that these materials can at least equal the penetration performance of conventionally alloyed tungsten penetrators. The current results do not offer evidence as to whether they hold promise for increased performance. Penetration of complex targets by these designs will present some problems, but based on the performance observed in these tests, an alternate lamination design, possibly but not necessarily of three-dimensional nature, may present a solution. Thus, the overall conclusion which I would draw from these results is that the concept of developing macro-composite or mechanically structured heavy alloy penetrators has feasibility.

These results are presented for your information and use in further materials development efforts in accordance with the terms of the SBIR contract between Applied Technology Associates and MTL. As further examination of these penetrators is done, I will inform you of the results. If you have any further questions regarding these tests, please contact either myself or Bob Dowding.

Sincerely,

Patrick Woolsey
Ballistic Impact Behavior Group

ENCL: DOP test data; plot
CF: R. Dowding, MEM
MDB File

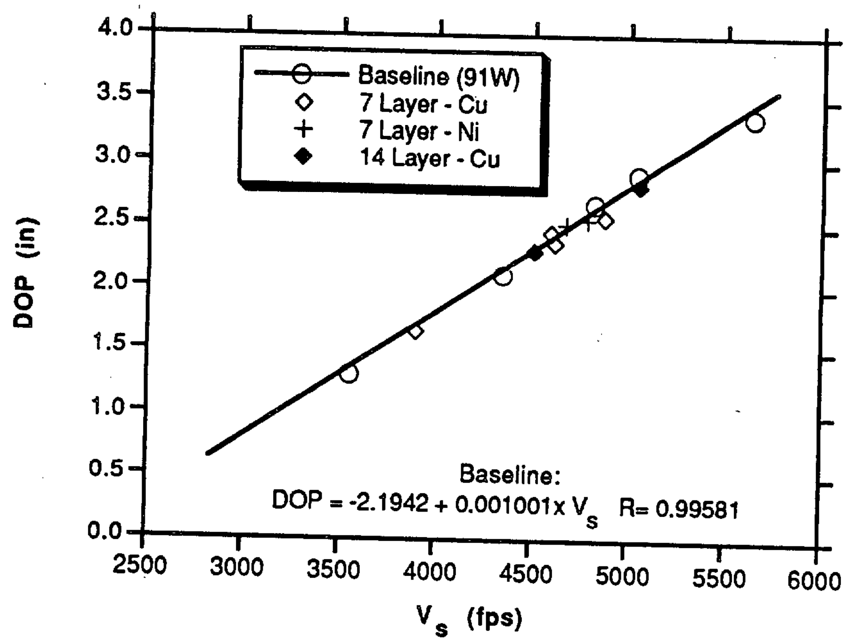

Figure 1. Penetration Efficiency Map for Laminated WHA Penetrators

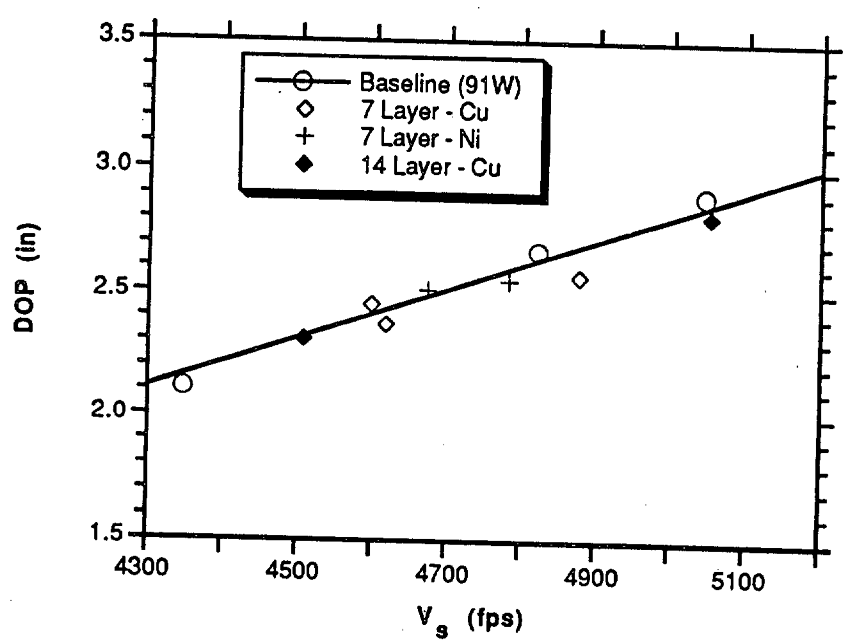

Figure 2. Complete Performance Plot for Laminated WHA Penetrators

Test No.	Penetrator	V_s (fps)	Yaw (°)	DOP (in)	DOP (mm)
T42-92-1*	90W laminate, 0.052", Cu; #1	4954	7.44	2.448	62.2
T42-92-2	90W laminate, 0.052", Cu; #2	4877	2.14	2.567	65.2
T42-92-3	90W laminate, 0.052", Cu; #3	4618	2.80	2.369	60.2
T42-92-4	90W laminate, 0.052", Cu; #4	4598	3.28	2.449	62.2
T42-92-5	90W laminate, 0.052", Cu; #5	3896	1.30	1.653	42.0
T44-92-1	90W laminate, 0.052", Ni; #9	4674	0.94	2.512	63.8
T44-92-2	90W laminate, 0.052", Ni; #10	4783	1.11	2.550	64.8
T45-92-1	90W laminate, 0.026", Cu; #11	5052	1.39	2.819	71.6
T45-92-2	90W laminate, 0.026", Cu; #12	4508	0.69	2.307	58.6

* - Unacceptable yaw

Table 1. DOP Tests (Semi-infinite Penetration)

Test No.	Penetrator	V_s (fps)	Yaw (°)	V_r (fps)	L_r (in)
T43-92-1	90W laminate, 0.052", Cu; #6	4893	3.42	3712	1.49
T43-92-2	90W laminate, 0.052", Cu, V-Notch; #7	4811	3.76	3863	1.64
T43-92-3	90W laminate, 0.052", Cu, V-Notch; #8	4873	3.79	3830	1.48
T52-92-1	91W, X-27C (1989)	4897	3.32	4314	1.60
T52-92-2	91W, X-27C (1989)	4845	2.77	3950	1.56

Table 2. A-Frame Oblique Plate Tests

Page intentionally blank

Distribution List

1 Office of the Secretary of Defense for Research and Engineering, The Pentagon, Washington, D.C. 20301

Director, U.S. Army Research Laboratory, 2800 Powder Mill Road, Adelphi, MD 20783-1197
1 ATTN: AMSRL-OP-CI-A
1 ATTN: Dr. Alan Goldman

Commander, Defense Technical Information Center, Cameron Station, Building 5, 5010 Duke Street, Alexandria, VA 22304-6145
1 DTIC-FDAC

1 MIAC/CINDAS, Purdue University, 2595 Yeager Road, West Lafayette, IN 47905

Commander, Army Research Office, P.O. Box 12211, Research Triangle Park, NC
27709-2211
1 ATTN: Information Processing Office
1 Dr. Andrew Crowson
Dr. Edward Chen

Commander U.S. Army Materiel Command (AMC), 5001 Eisenhower Avenue, Alexandria, VA 22333
1 ATTN: AMCSCI

Commander, U.S. Army Materiel Systems Analysis Activity, Aberdeen Proving Ground, MD 21005
1 ATTN: AMXSY-MP, Director

Commander, U.S. Army Missile Command, Redstone Scientific Information Center, Redstone Arsenal, AL 35898-5241
1 ATTN: AMSMI-RD-CS-R/Doc

Commander, U.S. Army Armament Research Development and Engineering Center, Dover, NJ 07801
1 ATTN: Technical Library
1 Mr. D. Kapoor
1 Dr. S. Cytron

Commander, U.S. Army Tank-Automotive Command, Warren, MI 48397-5000
2 ATTN: AMSTA-TSL Technical Library

Commander, U.S. Army Foreign Science and Technology Center, 220 7th Street, N.E., Charlottesville, VA 22901
3 ATTN: AIFRTC, Applied Technologies Branch, Gerald Schlesinger

Naval Research Laboratory, Washington, D.C. 20375
1 ATTN: Code 5830
1 Code 2627
1 Dr. Virgil Provenzano

Chief of Naval Research, Arlington, VA 22217
1 ATTN: Code 471

Naval Surface Weapons Center, Dahlgren Laboratory, Dahlgren, VA 22448
1 ATTN: Code G-32, Ammunition Branch, Mr. Brian Sabourin

Commander, Rock Island Arsenal, Rock Island, IL 61299-6000
1 ATTN: SMCRI-SEM-T

Battelle Columbus Laboratories, Battelle Memorial Institute, 505 King Avenue, Columbus, OH 43201
1 ATTN: Mr. Henry Cialone
1 Dr. Alan Clauer

Battelle Pacific Northwest Laboratories, P.O. Box 999, Richland, WA 99352
1 ATTN: Mr. William Gurwell
1 Dr. Gordon Dudder
1 Mr. Curt Lavender

GTE Sylvania, Inc. Chemical and Metallurgical Division, Hawes Street, Towanda, PA 18848
1 ATTN: Dr. James Mullendore
1 Mr. James Spencer
1 Ms. Susan Doepker

Director, Ballistic Research Laboratory, Aberdeen Proving Ground, MD 21005
1 ATTN: SLCBR-TSB-S (STINFO)
1 SLCBR-TB-P, Mr. Lee Magness
1 Ms. W.A. Leonard

Teledyne Firth Sterling, 1 Teledyne Place, LaVergne, TN 37086
1 ATTN: Dr. Steven Caldwell

Los Alamos National Laboratory, ATAC, MS F681, P.O. Box 1663, Los Alamos, NM 87545
1 ATTN: Mr. Bill Hogan
1 Mr. Paul Dunn
1 Mr. Bill Baker

Philips Elmet, 1560 Lisbon Road, Lewiston, ME 04240
1 ATTN: Mr. James Anderson

Ultramet, Inc., 12173 Montague Street, Pacoima, CA 91331
1 ATTN: Dr. J.J. Stiglich
1 Mr. Brian Williams
1 Dr. Robert Tuffias

Ceracon, Inc., 1101 N. Market Boulevard, Suite 9, Sacramento, CA 95834
1 ATTN: Dr. Ramas Raman
1 Mr. Sundeep Rele

Southwest Research Institute, 6220 Culebra Road, P.O. Drawer 28510, San Antonio, TX 78228-0510
1 ATTN: Dr. James Lankford

Metalworking Technology, Inc., 1450 Scalp Avenue, Johnstown, PA 15904
1 ATTN: Mr. C. Buck Skena
1 Mr. Timothy McCabe

Research Triangle Institute, P.O. Box 12194, Research Triangle Park, NC 27709-2154
1 ATTN: Dr. John B. Posthill

3C Systems, 620 Arglye Road, Wynnewood, PA 19096
1 ATTN: Mr. Murray Kornhauser

Advance Technology Coatings, 300 Blue Smoke Ct. West, Fort Worth, TX 76105

Alliant Techsystems, 7225 Northland Drive, Brooklyn Park, MN 55428
1 ATTN: Dr. Stan Nelson
1 Mr. Mark Jones
1 Mr. Thomas Steigauf

CAMDEC, 3002 Dow Avenue, Suite 110, Tustin, CA 92680

Chamberlain Manufacturing Co., 550 Esther St., P.O. Box 2545, Waterloo, IA 50704
1 ATTN: Mr. Tom Lynch

Defense Technology International, Inc., The Stark House, 22 Concord Street, Nashua, NH
1 ATTN: Mr. Douglas Ayer

Materials and Electrochemical Research Corporation, 7960 S. Kolb Road, Tucson, AZ 85706
1 ATTN: Dr. James Withers
1 Dr. Sumit Guha

Materials Modification, Inc., 2929-P1 Eskridge Center, Fairfax, VA 22031
1 ATTN: Dr. T.S. Sudarshan

Micro Materials Technology, 120-D Research Drive, Milford, CT 06460
1 ATTN: Dr. Richard Cheney

Nuclear Metals, 2229 Main Street, Concord, MA 01742
1 ATTN: Dr. Willian Nachtrab

Olin Ordnance, 10101 9th Street N., St. Petersburg, FL
1 ATTN: Hugh McElroy

The Pennsylvania State University, Department of Engineering Science and Mechanics, 227 Hammond Building, University Park, PA 16802-1401
1 ATTN: Dr. Randall M. German, Professor, Brush Chair in Materials

Worcester Polytechnic Institute, 100 Institute Road, Worcester, MA, 01609
1 ATTN: Dr. Ronald Biederman
1 Dr. Richard Sisson

Failure Analysis Associates, Inc., 149 Commonwealth Drive, PO Box 3015, Menlo Park, CA 94025
1 ATTN: S.P. Andrew
1 R.D. Caliguri
1 T.K. Parnell
1 L.E. Eiselstein

Amorphous Technologies International, Laguna Hills, CA
1 ATTN: Mr. Dick Harlow

Parmatech Corporation, 2221 Pine View Way, Petaluma, CA 94952
1 ATTN: Dr. Animesh Bose

Director, U.S. Army Research Laboratory, Watertown, MA 02172-0001
2 ATTN: AMSRL-OP-CI-D, Technical Library
1 AMSRL-OP-CI-D, Visual Information
1 AMSRL-OP-PR-WT
20 AMSRL-MA-MB, Mr. Robert Dowding COR